CHARACTERIZATION AND DISCRIMINATION OF SELECTED VEGETATION CANOPIES FROM FIELD OBSERVATIONS OF BIDIRECTIONAL REFLECTANCES

by
Sheila Donovan

Thesis submitted to the Faculty of the Graduate School
of the University of Maryland in partial fulfillment
of the requirements for the degree of
Master of Arts
1985

ACKNOWLEDGEMENTS

The author wishes to express her sincere appreciation for the assistance given by Dr. Donald Deering, Ms. Betsy Middleton and Mr. Thomas Eck of the Earth Resources Branch of the NASA Goddard Space Flight Center. A particular word of thanks goes to Drs. Samuel Goward and Donald Petzold of the Department of Geography, University of Maryland, for their encouragement and supervision throughout this project. The helpful suggestions made by Dr. Michael Kearney of the previously mentioned department are also gratefully acknowledged.

CURRICULUM VITAE

Name: Sheila Marie Donovan.

Permanent address: 370 Village Street, Medway, MA. 02053.

Degree and date to be conferred: M.A., 1985.

Date of birth: [redacted]

Place of birth: [redacted]

Secondary education: Quincy High School, Quincy, MA., 1971.

Collegiate institutions attended	Dates	Degree	Date of Degree
Quincy Junior College	9/71-5/73	-	-
Northern Arizona University	8/77-5/79	B.S.	1979
Northern Arizona University	1/81-12/82	B.S.	1982
University of Maryland	8/83-12/85	M.A.	1985

Major: Geography.

ABSTRACT

Title of Thesis: Characterization and Discrimination of Selected Vegetation Canopies From Field Observations of Bidirectional Reflectances

Sheila Marie Donovan, Master of Arts, 1985

Thesis directed by: Dr. Samuel N. Goward, Asst. Research Scholar, Department of Geography

A full evaluation of the bidirectional reflectance properties of different vegetated surfaces has been limited in past studies by instrumental inadequacies. With the development of a new instrument, the PARABOLA, it is now possible to sample reflectances from a large number of view angles in a short period of time, maintaining an almost constant solar zenith angle. PARABOLA data collected over five different canopies in Texas are analyzed in this study, this being one of the first full evaluations of data from this instrument.

The objectives of this investigation were to evaluate the inter-canopy and intra-canopy differences in bidirectional reflectance patterns. Particular attention was given to the separability of canopy types using different view angles for the red and NIR spectral bands. Comparisons were repeated for different solar zenith angles. Statistical and other quantitative techniques were used to assess these differences.

For the canopies investigated, the greatest reflectances were found in the backscatter direction for both spectral bands. Canopy discrimination was found to vary with both view angle and the spectral reflectance band considered, the forward scatter view angles being

most suited to observations in the NIR and backscatter view angles giving better results in the red band. Because of different leaf angle distribution characteristics, discrimination was found to be better at small solar zenith angles in both spectral bands.

APPROVAL SHEET

Title of Thesis: Characterization and Discrimination of Selected Vegetation Canopies From Field Observations of Bidirectional Reflectances

Name of Candidate: Sheila Donovan
Master of Arts, 1985

Thesis and Abstract Approved: _____
Dr. Samuel N. Goward
Assistant Research Scholar
Department of Geography

Date Approved: _____

TABLE OF CONTENTS

TABLE OF CONTENTS (continued)

TABLE OF CONTENTS (continued)

LIST OF TABLES

LIST OF FIGURES

1 INTRODUCTION

A relatively unexploited aspect of remote sensing is off-nadir viewing of the earth's features from aircraft, satellites and ground-based sensors. However, National Oceanic and Atmospheric Administration's (NOAA) Advanced Very High Resolution Radiometer (AVHRR) scans plus and minus 56 degrees of nadir and future systems like Satellite Probabatoire pour L'Observation de la Terre (SPOT-1), will have pointable view angle capabilities. The potential increase of temporal and spatial coverage resulting from off-nadir viewing is considered a major advantage of directional off-nadir measurements (Schnetzler, 1981). However, before this additional source of data can be used with confidence, the effects and possible advantages of off-nadir viewing and changing solar zenith angles need to be known.

Until recently, reflectances of earth surfaces were assumed to be isotropic, mainly because remote sensing systems have typically collected measurements only from nadir with a restricted field-of-view. Thus, the variability that occurs with changing view angle and solar zenith angle had not been recognized because nadir

observations and constant times of observations resulted in apparently similar reflectances. The interaction of radiation with vegetation is now known to be a complex relationship that is a function of canopy structure and optics, solar zenith and view angle. Theoretically, this interaction is represented by the bidirectional reflectance distribution function (BRDF). However, in practice the bidirectional reflectance factor (BRF) is usually determined by a ratio of radiation reflected from a target to that reflected by a perfectly diffuse lambertian surface.

Most bidirectional reflectance reseach has been limited to simulation models because of the difficulty in collecting field data. Although only a few directional reflectance distributions covering the entire hemisphere of earth surfaces have been collected (Smith and Ranson, 1979), the potential of using off-nadir measurements as a source of information has been demonstrated by Kimes (1983) and Barnsley (1984). Research generally has shown that lowest reflectances occur near nadir and increase with off-nadir viewing. In addition, variations in reflectance with changing solar zenith angles have also been shown.

The nature of bidirectional reflectance suggests bidirectional reflectances have unique characteristics associated with different vegetation cover types and these characteristics may be used to discriminate cover types, thus increasing classification accuracy. A number of studies, using simulation models and observations collected from aircraft, have indicated that increased classification accuracy would result from the use of off-nadir view angles. Despite these findings based on modeled reflectances, there is still a need for empirical studies to verify these theoretical results. However, the effect on discrimination of off-nadir observations collected from ground-based sensors has not been addressed in the literature. The length of time required to obtain sufficient samples at different view angles by typical ground-based sensors makes observations of BRF for constant solar angles difficult. However, a recent technological advance in research instrumentation has led to the development of the Portable Apparatus for Rapid Acquisition of Bidirectional Observation of the Land and Atmosphere (PARABOLA) which makes it possible for the rapid sampling of the entire ground hemisphere at specified view angles.

This study will use PARABOLA observations to investigate the potential of bidirectional reflectance for the discrimination of vegetation canopies. A statistical test, the t-test, is used to analyze intercanopy reflectance in two areas: 1) the differences in reflectances between nadir and off-nadir view angles for different solar zenith angles, and 2) reflectance variability between solar zenith angles at selected view angles. The t-test will also be used to test the significance of reflectance differences between different canopy types for varying view and solar zenith angles. The differences in reflectance between canopies is quantified in feature space by using Euclidean distances between the mean reflectance values of each canopy cover.

This is the first attempt at using ground-based observations for the purpose of feature discrimination. As a result, the study is not exhaustive but is a preliminary investigation conducted using some of the first data from the PARABOLA. However, it is the intention of this study to provide results which may give an indication as to the utility of off-nadir observations and potential problems and areas of future research.

2 LITERATURE REVIEW

The past emphasis in remote sensing has been to improve spatial, radiometric and spectral resolutions. These improvements have led to a tremendous increase in data and were expected to significantly improve the information content of the reflectance data. However, an analysis of classification accuracies, which should result from increased information content, have not occurred.

Emphasis has shifted recently to researching the effects of off-nadir viewing on surface reflectance. The bidirectional reflectance properties about the surface have been virtually ignored in terms of contributing and understanding remote sensing data. The complicated relationship between solar radiation and surface features have made field studies difficult while models simulating bidirectional reflectances have had limited success. A brief review of the effects of resolution improvements on discrimination is given followed by a detailed discussion of bidirectional reflectance and its effect on discrimination.

2.1 Effects of Remote Sensing Resolution Advancements on Discrimination

With the launching of the first Landsat satellite in 1972, detailed repetitive spectral data of the earth was obtained for the first time. Experiments designed by NASA in the 1970's successfully used landsat Multispectral Scanner (MSS) data to test the ability of remote sensing to assess worldwide agricultural production. Consistently high classification accuracies were reported throughout the experiments. However, classification accuracies from landsat data reported in the literature have not been as successful as the NASA experiments had at first indicated. For example, a statistical survey of 224 Landsat investigations by Jayroe (1978) reported an average accuracy of 74 percent when compared to ground-based studies for crop inventory. This study also reported an average accuracy for crop classification mapping of 63 percent. Varied accuracies also were reported by Fan (1979) depending on type of imagery and classification categories. For Landsat 1 MSS data an 83 percent average accuracy for urban landuse was reported.

In July, 1982 Landsat 4 was successfully launched

with a MSS and new, advanced sensor, the Thematic Mapper (TM), on board. The TM represents results of a research and development effort in which major improvements in remote sensing since the MSS have been simultanuously intergrated into one system (Williams et al., 1984). Specific improvements over the MSS have been achieved in spatial (80 to 30 meters), radiometric (6 to 8 bits), and spectral (4 to 7 bands) resolutions. The additional spectral bands were specifically chosen to maximize vegetation discrimination while improved spatial resolution was expected to significantly increase classification accuracy.

Studies by Williams et al. (1984) and Irons et al. (1984) attempted to identify the contribution of the individual sensor parameters from recently acquired TM data. An analysis of variance approach was used to isolate effects of spatial, spectral and radiometric improvements over MSS data. Spatial resolution was found to be statistically insignificant for improving classification accuracy in the Williams et al. (1984) study and to consistently decrease in the study by Irons et al. (1984). These results substantiate earlier findings (Dean and Hoffer,1982, Latty and Hoffer,1981, and

Sadowski et al.,1977) obtained from simulation studies, namely, that the significant improvement in spatial resolution has had little positive impact on classification accuracy.

In analysis of radiometric and spectral resolution improvements of TM data, conflicting results were reported by Williams et al.(1984) and Irons et al.(1984). Williams et al. (1984) showed 3-8 percent increase in classification for radiometric and spectral resolution increases. The Irons et al. (1984) study was conducted on two different TM scenes, urban and agricultural, with results suggesting these improvements are highly dependent on spectral and spatial scene attributes. Improvements in classification accuracy of approximately 5 percent were found for radiometric and spectral resolution on the urban scene while no significant effect occurred for the agricultural scene.

2.2 Bidirectional Reflectance Effects on Vegetated Surfaces

2.2.1 Early Studies

Most remote sensing systems , such as the MSS and TM, only collect measurements from the nadir position. Until the mid-1960s the nadir view angle was thought to characterize accurately hemispherical reflectance since surface reflectance was considered to be isotropic. The anisotropic nature of surface reflectance in different wavelengths had not been recognized because routine observations maintained a constant nadir view and time of observation resulting in apparently similar reflectances of given surfaces.

Although a few studies (Krinov, 1947, and Coulson, 1956) had shown variation in reflection with different wavelengths, it was not until the 1960s that researchers seriously investigated the assumption of isotropic reflectance of surfaces. In calculating albedo from satellite data, researchers discovered that albedo measurements were found to be consistently low (Salomonson, 1966). In a laboratory study on natural surfaces, Coulson (1966) investigated the possible reasons

for low albedo measurements. He found that by varying view angles from the nadir position minimum reflectance off surfaces occurred in the nadir region with increasing reflectance occurring with increasing view angle. If this trend applies to most surface reflectance, then the calculated hemispherical reflectance would be underestimated resulting in the low albedo measurements.

Coulson (1966) suggested that reflected solar radiation was a function of wavelength, solar zenith angle, view angle and optical properties of the atmosphere and surface. He saw the need for more studies on the variation of reflection with angle, saying that little work had been done on the subject. Salomonson (1966) provided early evidence of the anisotropic characteristic nature of the earth's surface by presenting results from aircraft radiometer measurements of reflected solar energy. Data collected over clouds, grassland, sand and ocean indicated that significant forward and backscattering occurred with increasing solar zenith angles. Coulson (1966) suggested that albedo estimates should take account of anisotropic characteristics of natural surfaces.

The anisotropic nature of solar reflectance from clouds, water, and land surface using an aircraft-mounted radiometer was investigated by Brennan and Bandeen (1970). Varying view angle and azimuth direction, data were collected in two bands, 0.55-0.85um and 0.2-4.0um. The results substantiated the findings of Coulson (1966) and Salomonson (1966) that found that natural surfaces are anisotropic with minimum reflectance at nadir with clouds, forests, and ocean showing similar bidirectional scattering patterns.

2.2.2 The Nature of Bidirectional Reflectance

Previous investigations of hemispherical canopy reflectance primarily relied on laboratory reflectance measurements of leaves. Researchers began to realize the limitation of this approach in understanding aircraft and satellite remote sensing data. Colwell (1974) emphasized the complicated relationship that exists in investigating reflected solar radiation. Characteristics of the canopy, background, solar zenith, look angle and azimuth should be understood to predict reflected solar radiation (Colwell, 1974). In modeling the reflectance of grasses, Colwell

(1974) examined the effects of these parameters concluding that all can vary at any given time but all should be considered important.

The first real investigation into isolating parameters thought to effect reflectance was attempted by Egbert and Ulaby (1972). To account for the anisotropic nature of surface reflectance, research was designed to predetermine optimal filter combinations in a multiband experiment. Analysis of reflectance measurements showed how target brightness and contrast can change as a function of viewing geometry. Grass canopies, dominated by vertical components, were found to have significant variations in reflectance as a function of look angle. Variations for certain combinations of solar zenith and azimuth were also found.

Nicodemus (1970) developed an expression to explain the anisotropic reflectance nature of the surface. The reflection properties of a surface are described by the bidirectional reflectance function (BRDF) defined as:

$$f(\theta,\phi,\theta',\phi') = \frac{dL'(\theta',\phi')\ sr^{-1}}{dE(\theta,\phi)}$$

Where:

θ = zenith angle of radiation source

ϕ = azimuth angle of radiation source

θ' = zenith angle of sensor

ϕ' = azimuth angle of sensor

dL' = reflected radiance in the direction

dE = incident radiation from the direction

sr^{-1} = steradian

Although mathematically and completely descriptive of a surface, BRDF is difficult to evaluate. It can not be measured directly because truely infinitesimal elements of solid angle do not include measureable amounts of radiant flux (Deering, 1984). Thus, BRDF is only a theoretical explanation of the surface interaction of reflection characteristics. In practice, the average of the BRDF over finite solid angles of incidence and exitance radiance is used. This average quantity is termed bidirectional reflectance factor (BRF) and is defined as the ratio of the radiant flux actually reflected and that reflected by a lambertian surface identically irradiated and observed (Nicodemus, 1977).

2.2.3 BRDF Simulation Models

Due to the difficulty of isolating and observing various characteristics under natural conditions, the use of mathematical simulation models was necessary (Kirchner et al., 1981). In these models, parameters that control canopy reflectance - leaf optics canopy geometry, background, azimuth angle, solar zenith and view angle - can be specified and may be varied independently to obtain reflectance as a function of canopy characteristics.

Suits (1972) developed the first model to predict the non- lambertian characteristic of vegetation canopies. The Suits model is basically an extension of the Allen, Gayle, Richardson (AGR) Model (1970). The AGR Model relates leaf area index (LAI) to hemispherical reflectance but does not account for reflectance variations as a function of view angle (Suits, 1972). The radiation interaction with plant canopies, based on spectral and geometric characteristics, results in predicted bidirectional reflectance. Analysis of simulated data demonstrated variation of reflectance as a function of view angle. Suits (1972) suggested that this variability be attributed to the ratio of vertical to horizontal

canopy components sensed with changing view angle.

The Solar Radiation Vegetation Canopy (SRVC) Model differs from the Suits Model, in that it is a stochastic rather than deterministic model of radiation interaction with plant canopies. The primary reasons a stochastic model is advantageous are that most remote sensing algorithms are stastically oriented and that reflectance processes are stochastic by nature (Smith and Oliver, 1972). The SRVC simulates the interaction of radiation in a multilayer canopy to determine directional reflectance by accounting for variations of sun angle, sensor view angle, canopy geometry and optical properties. Basically, each iteration through the model consists of the probability of flux from any given source entering the canopy and hitting a gap in the layered canopy. Sufficient interations results in statistics that can be useful in various algorithms.

Most recent simulation studies have used the SRVC Model to understand the behavior of vegetation canopy as a function of solar zenith and view angles. Kimes et al. (1980) studied solar zenith effects on contrasting geometric structures. Spectral reflectance was found to

increase with increasing solar zenith angle on an erectophile and planophile canopy. Smith (1975) showed that spectral reflectance can both increase or decrease depending on the type of the crop and developmental stage. The effects of varying azimuth, solar and view angles were modeled on seven vegetation canopies in bands .68um (red) and .80um (NIR) by Kirchner et al. (1981). Analysis of the data showed that at 0.68um there was much more variability than at 0.80um within a 35 degree view angle with radiances varying from 25 percent less to 35 percent more than at nadir while there was only plus or minus 5 percent variability at 0.80um. In addition to the previously observed trend of increasing reflectance with increasing solar zenith angle, variability also is shown to decrease with increasing biomass.

2.2.4 Field Studies of BRF

Plant canopy reflectance models had limited success in predicting detailed spectral reflectance. Yet until the late 1970s only a few directional reflectance distributions covering the entire hemisphere of vegetation had been measured and little analysis performed (Smith and

Ranson, 1979). This was understandable as the BRDF is a complex function of variables such as geometric structure of the vegetation and soils, optical properties, background, solar zenith, azimuth and view angle. However, within the last five years, research has focused on BRDF field work to extract unique information about physical properties of natural surfaces and also to improve interpretation of aircraft and satellite data that have off-nadir sensors.

The objective of applying remote sensing in agriculture has encouraged recent studies of the bidirectional reflectance properties of agricultural crops (Staenz et al., 1981). Although research has shown that target radiance varies with view and solar angles, only recently have efforts been made to relate BRF observations at various illumination and viewing geometries to the structural properties of vegetation. Field work on agricultural crops has illustrated additional problems in interpretation of BRF values. Ranson et al. (1981) using a truck- mounted radiometer measuring in the visible and NIR wavelengths related changes of LAI, leaf inclination and percent cover in soybeans to reflectance values. Well-developed canopies in NIR and visible showed little

effect with varying solar zenith angles. However, in canopies with well-developed row structure, reflectance was strongly affected by solar zenith changes in the visible band but less so in the NIR. Ranson et al. (1981) suggested that shadows cast by rows strongly influence reflectance values thus posing a significant interpretation problem.

Kirchner et al. (1982) eliminated the problem of row structure in studying an alfalfa crop which shows no pronounced row structure. In this study, research illustrates the rates of change of a crop as a function of geometric structure, solar zenith and view angle (Kirchner et al. ,1982). In the early stages of development, alfalfa is characterized by low biomass and an erectophile structure. As a result of these characteristics, solar angle changes result in considerable variations in reflectance, but reflectance stabilizes with plant maturity as the structure becomes planophile with high biomass. In general, the variability of reflectance with view angle was found to decrease as the biomass increases. However, this decrease in variability of reflectance with crop maturity still resulted in doubling of percent change in reflectance with view angles extended to 45 degrees for

both the visible and NIR bands.

Trends, similar to those shown by Kirchner et al.(1982), were observed by Kimes (1983) and Kirchner et al. (1980) , in field studies on vegetation canopies. As reported in Kirchner et al. (1982), complete homogeneous vegetation reflectance increases as off-nadir viewing increases for all azimuth view and solar angles. This trend is attributed to the shading of lower canopy layers by the upper layers and by viewing different proportions of the layers as view angle changes (Kimes, 1983). Sparse canopies are found to exhibit the same variability with changing solar zenith angle in the visible wavelengths due to strong backscattering toward the sun. In the NIR the same trends occur as for complete canopies in the visible, but the strong backscattering by soil has substantially less effect. However,results from Barnsley (1984) indicate greatest view angle effects in the NIR wavelengths which contradict the results from Kimes et al. (1983) and Kirchner et al. (1982). Barnsley attributes this discrepancy to intergration caused by using broad bands.

2.2.5 Improved Classification using Bidirectional Reflectance Observations

Previous studies suggest that directional reflectance measurements of vegetation canopies and agricultural crops have unique characteristics which can be used to distinguish between different cover types (eg. Kimes et al.,1984, Kirchner et al.,1982). Modeling of the radiation interaction with plant canopies was first initiated as a potential tool for improving the recognition process by Smith and Oliver (1974). They recognized the significance of variation of reflectance with view angle for discrimination of vegetation canopies. Smith and Oliver (1974) used the SRVC model to investigate the effects of directional reflectance characteristics on discrimination. In this study on shortgrass prairie , spectral signatures were calculated as a function of view angle for two hypothetical canopies that have different leaf area indices. Iterations through the model permit calculation of mean vectors and covariance matrices for reflectance at different sensor view angles. These statistics are used to calculate divergence between targets for different wavelength combinations. Seven wavelengths between .4-.7um, showed that different pairs

of wavelengths discriminate better than others and that some targets show greater separability at some scan angles (Smith and Oliver, 1974). These results indicate that combinations of different wavelengths and view angles can be expected to increase classification accuracy.

Although studies by Egbert and Ulaby (1972), Kirchner et al. (1982) and Kimes et al. (1984) have suggested that bidirectional reflectance measurements may improve feature discrimination, no direct attempt was made to prove this hypothesis until the examination of MSS data by Ott et al. (1984). In analysis of MSS data with a scan angle of plus or minus 50 degrees, the authors take into account angle dependent effects using a maximum liklihood classification. Comparision between a classification using an entire scan angle and an angle-dependent classification show a significant overall increase in classification accuracy from 74 to 90 percent (Ott et al.,1984).

Basic and applied research into the contributions bidirectional reflectance can make in increasing discrimination have been hampered largely by instrument limitations. However, recent developments have

circumvented many of the early problems associated with collecting bidirectional reflectance measurements and there is now a growing body of research addressing the problems and fundamental nature of bidirectional reflectance of surfaces.

The study presented here is a pilot investigation of the effects of off-nadir viewing and solar zenith angles on the discrimination of selected vegetation cover types using state-of-the-art instrumentation. The potential for using off-nadir observations in remote sensing applications is considered. The specific objectives of this investigation are outlined in the section that follows.

2.3 Objectives

The utilization of remotely sensed data for geographic applications has primarily been directed at the discrimination and classification of earth features. However, the full potential of these data for geographic applications has, as yet, not been realized because most analytical techniques are based on nadir observations and

the assumption that surfaces are isotropic reflectors. As indicated earlier, a number of recent studies have revealed the anisotropic nature of natural surface covers and the potential for enhanced feature discrimination using off-nadir observations (e.g. Kimes, 1983).

The underlying aim of this investigation is to evaluate field collected bidirectional reflectance data in terms of its potential for discriminating selected canopy covers. More specifically, the objectives are to: 1) determine the nature of bidirectional reflectance distributions of each canopy in both the red and NIR spectral bands at selected solar zenith angles. This analysis is intended to reveal any unique reflectance properties which may be displayed by each canopy. Such properties would be useful for canopy discrimination based on spectral reflectance characterisitics, and 2) evaluate bidirectional reflectance data using quantitative methods to determine the most suitable view angles or view angle combinations for a given spectral band and solar zenith angle for the optimum discrimination of canopy pairs.

3 METHODOLOGY

3.1 Instrumentation

The PARABOLA was designed specifically for fundamental research of bidirectional reflectance (Deering, 1984). The instrumentation was designed with five important attributes: rapid sampling, good radiometric sensitivity, self-contained data acquisition system, portability and rugged design for field use and a multiple platform mounting capability (Deering,1984). Previously, the major obstacle to field collection had been the lack of a rapid sampling ability for off-nadir measurements. Rapid sampling effectively minimizes changing solar position and sky conditions during the sampling procedure. The additional improvements of infield mobility and mounted calibration also provide significant improvement over previous field sampling techniques.

The PARABOLA is essentially a 3-channel rotating head radiometer and data recording unit designed for use on a variety of platforms. Although this instrument was built originally for support by a tripod mount, other platforms have been used including a Goddard Space Flight Center

Instrument van, hot-air ballon and Transportable Pickup Mount System (TPMS). TPMS, the support vehicle used for this study , consists of a light-weight, collapsable boom that mounts on a pick-up truck as illustrated in Fig.3.1, thus allowing sampling under most field conditions.

The three detectors mounted on the radiometer cover the spectral bands 0.65-0.67um (red), 0.81-0.84um (NIR) and 1.62-1.69um (SWIR) that approximate TM bands 3,4,and 5. However, the bands can be changed or adjusted to desired specifications. Two of the three detectors are silicon photodiodes for the visible-NIR part of the spectrum and germanium photodiode designed for the mid-infrared spectral range, are defined by narrow band interference filters.

The radiometer, mounted 518cm above the ground, samples radiation fluxes from the detectors simulteanously in 15 degree view angle increments and approximately 30 degree increments of view azimuth. The sampling scan of the entire ground-sky sphere results in 263 samples for each channel per scan cycle as illustrated in Fig. 3.2. The data set, taken in an 11-second period, is followed by a 35-second transfer to a tape recorder of voltages

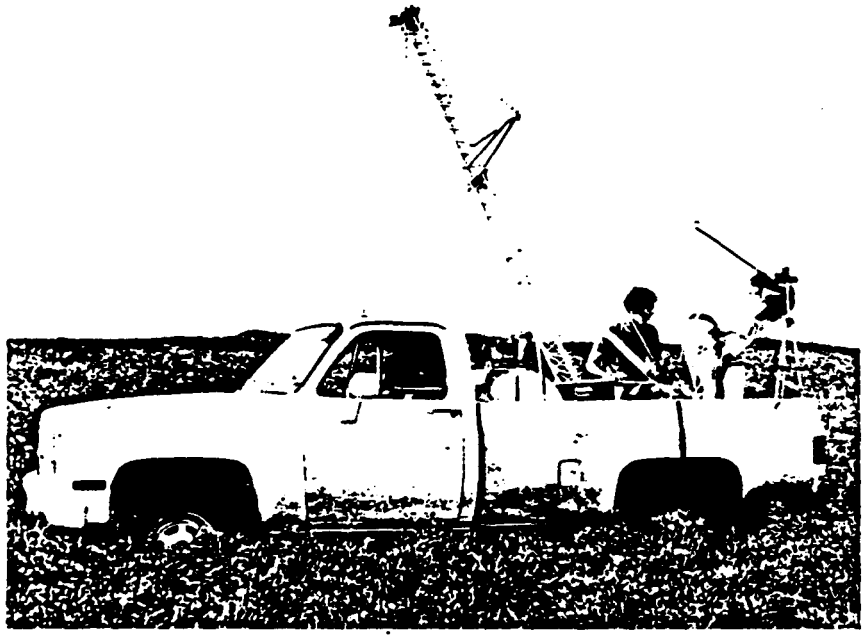

3.1 PARABOLA with Transportable Pickup Mount System (TPMS) (Source: Deering, 1984).

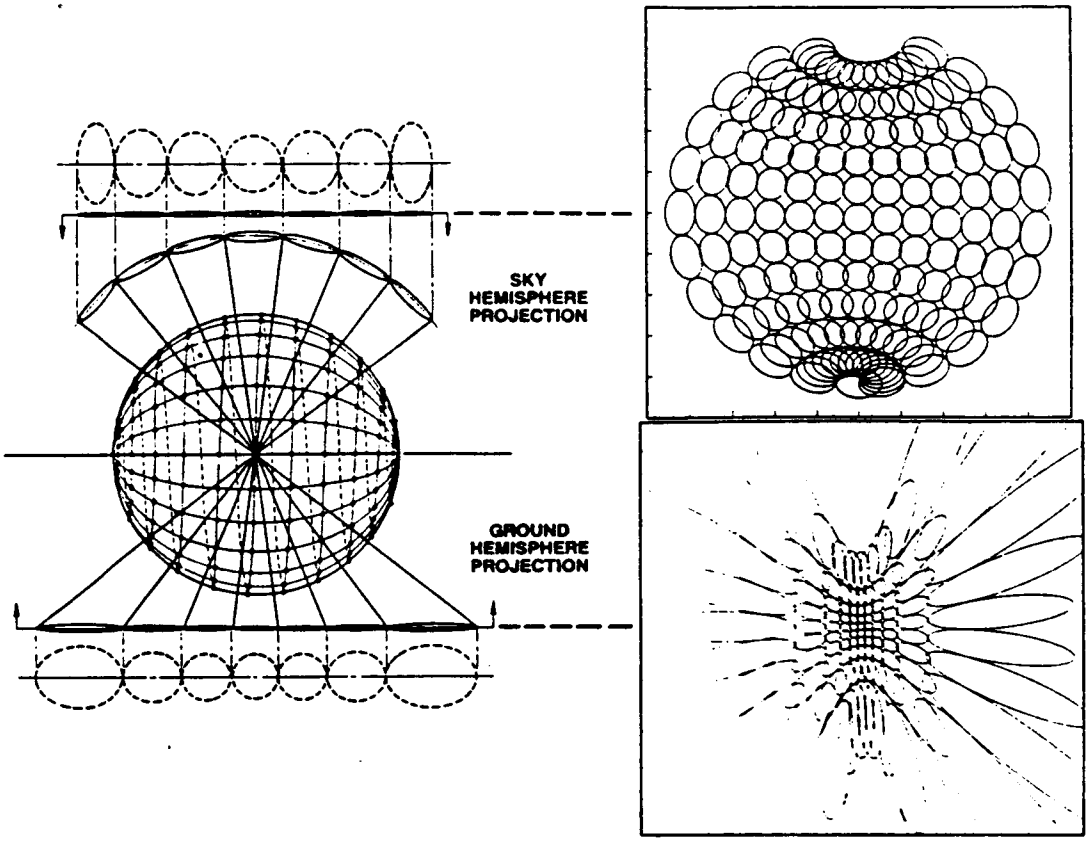

3.2 PARABOLA instanteaneous field of view (IFOV) pixels projected onto a two-dimensional surface (Source: Deering, 1984).

produced by the PARABOLA. These voltages are later transformed to reflectance using the calibration procedure described in section 3.4.1.

For this research only observations in the principle plane of the sun were analyzed. The principle plane is the direction of the sensor looking toward the sun (azimuth 0 degrees) and directly away from the sun (azimuth 180 degrees). Thus an azimuth of 0 and 180 degrees represents forward and backscattering respectively. Kimes (1983) shows that the major peaks and mininum reflectance that occur in the principle plane, adequately characterize directional reflectance of homogeneous canopies.

3.1.1 Assumptions and Limitations

Although the PARABOLA has improved significantly field sampling techniques, engineering restrictions prevent the PARABOLA from sampling the same ground pixel. Fig. 3.2 indicates that for every change in view angle and azimuth direction a different area on the ground is viewed. Therefore, it must be assumed that spatial

homogeneity exists for any interpretation of the PARABOLA data. There are several checks which may be performed to establish the degree of homogeneity of vegetation types in this study.

An initial qualitative assessment of spatial homogeneity is made in selection of each study site. An area approximately 30m by 30m was needed to cover the full scan of the PARABOLA. Site selection was guided by consistency in vegetation heights and the spacing between plants.

Due to the constant change in solar position, data sampling was restricted to less than 15 minutes duration. Thus, samples within a number of distinct solar zenith angles were collected. Within this period of time five samples were collected. Repositioning of the TPMS for each sample prevented more samples from being collected in a 15 minute period. The five samples for each solar zenith angle, in addition to pixel size, which averages greater than 3.35 square meters, was assumed to represent adequately vegetative variability (Deering, 1985; Personal communication).

A more quantitative measure of homogeneity was achieved by performing the F-Test which is described in detail in Section 3.5.3. The F-test is used here to test for equal variance within each cover type by comparison of view angle means. Since the PARABOLA is a rotating scanner, each view angle looks at representing different areas of the sample site, thus the spatial homogeneity of each cover type is tested by this analysis.

3.1.2 Pixel Size

The rotating radiometer head results in data collected from a variety of ellipsoid shapes and pixel sizes. At the nadir position, the pixels are circular and become increasingly ellipsoid and larger as the off-nadir angle increases as is illustrated in Fig. 3.3 . Pixel size, determined by the height of the PARABOLA above the canopy and the instanteaneous field of view (IFOV), may be calculated for off-nadir pixels from:

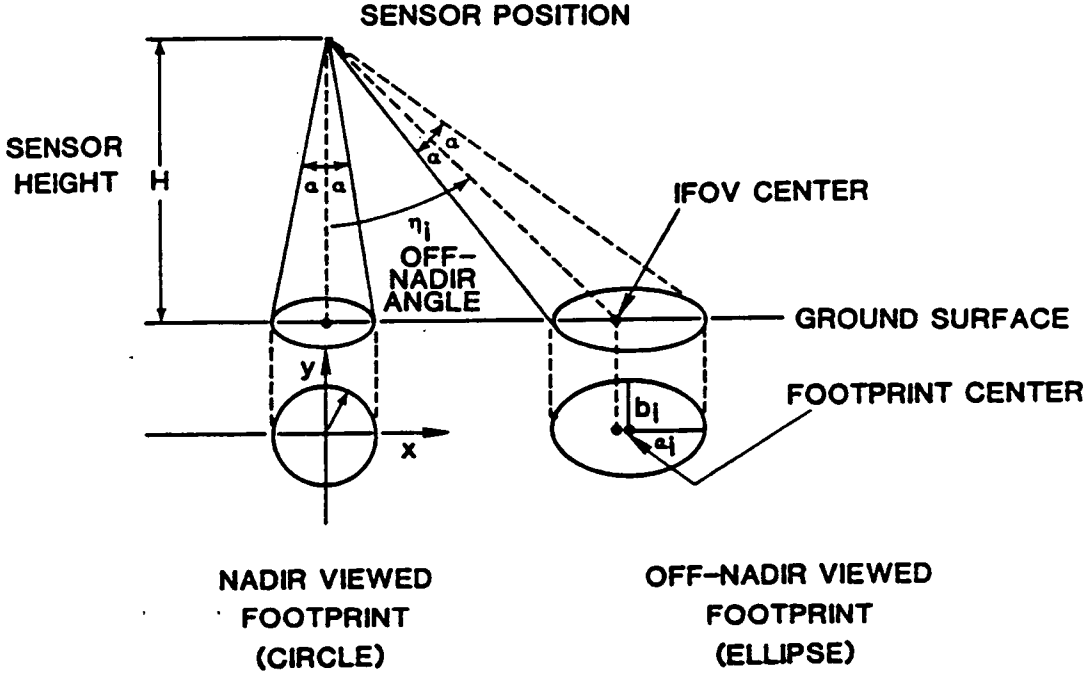

3.3 Projected footprints (pixels) of the PARABOLA IFOV on the surface (Source: Deering, 1984).

$$f(\Theta,\phi,\Theta',\phi') = \frac{dL'(\Theta',\phi')}{dE(\Theta,\phi)} \quad sr^{-1}$$

Where:

A_i = area of the ellipsoid

a_i = major axis and is defined as:

a_i = Htan (1+tan N)/1-(tan tanN)

Where:

H = sensor height above canopy

N_i = off-nadir angle

α = 1/2 the IFOV

B_i = minor axis and is defined as:

B_i = Htan /cosN 1-(tan tanN)1/2

and for nadir from:

$$2\pi r^2 = A_i$$

3.1.3 Support Instrumentation

Supporting instrumentation for the experiment includes a fish-eye camera mounted adjacent to the radiometer on the PARABOLA for ground documentation, a truck-mounted fish-eye lens camera for sky conditions and a sun photometer. For each sampling sequence, the two

cameras recorded sky condition and surface features simulteanously thereby, providing photographic verification of the measurements. The sun photometer, recording intensity of direct solar radiation in narrow wavelength bands, is used to calculate irradiance. The sun photometer is described in further detail in the calibration section.

3.2 Study Sites

A preliminary research effort to collect PARABOLA data in West Texas (Fig. 3.4) was undertaken in September, 1985. The objective of the experiment was to collect PARABOLA data of homogeneous vegetation types representative of a semi-arid environment. The semi-desert grasslands of southwest Texas and the southern high plains of Northern Texas were selected as study sites to sample representative vegetation types.

3.2.1 Vegetation Sampling Sites in the Semi-desert Grasslands

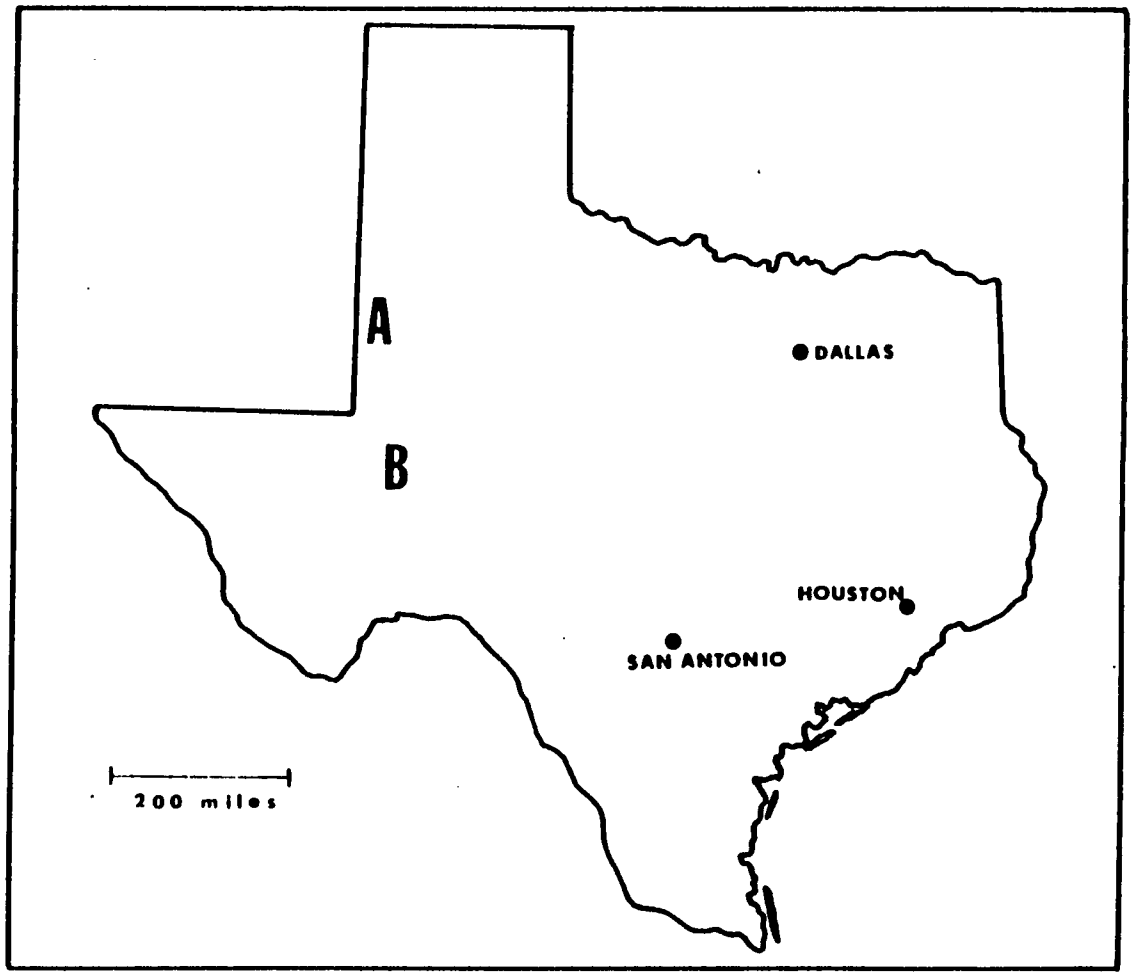

3.4 Location of the semi-desert grasslands (A) and the southern high plains (B) study sites in Texas.

The grasslands of the semi-desert lands (Southwest Texas, Southeast Arizona and Southern New Mexico) have given way to higher densities of shrubs during the past 75 years (Wright and Bailey, 1982). Since climatic change has not been sufficient to account for this vegetation succession, lack of fires, drought and overgrazing are believed to be responsible for the changing vegetation (Wright and Bailey, 1982).

Cresote bush (Larrea tridentata) and rough coldenia (Coldenia hispidissima) are two of the vegetation types sampled within the semi-desert grasslands. Background information relating to vegetation characteristics of the semi-desert grasslands and the southern high plains are summarized in Table 3.1 and 3.2. Creosote is major invader into the semi-desert grasslands as a result of overgrazing. Rough coldenia, a thinly spaced shrub, occupies a small portion of the area. Creosote bush and rough coldenia occur in gypsum range areas that consist of loamy soils varying in depth and underlain by white gypsic earth (Dittemore and Moore, 1964). These plants must be tolerant of gypsum and dry soil, with the invading plant determined by the depth and particular soil type.

Table 3.1 Canopy characteristics of selected vegetation types.

Common name (species)	Height	Spacing	Slope	Plant density	Biomass** wet/dry	Soil background	Plant description
Creosote bush (Larrea tridentata)	76.2cm	152.4cm	0-1%	14.7%	650/533	McCarran series, calcareous and gypsceous loamy soils	Large, woody shrub, darkgreen to yellow-green glossy leaves
Rough coldenia (Coldenia hispidissima)	12.7cm	60.9cm	0-1%	18.4%	140/33	McCarran series, calcareous and gypsous loamy soils	Small, woody shrub, slender stems, no green biomass
Shinnery oak (Quercus havardii)	43.1cm	15.2cm	0-3%	48.5%	594/439	Tivoli series, deep, light-colored, loose sands	Woody shrub with dark-green glossy leaves
Broom snakeweed (Xanthocephalum sarathrae)	20.3cm	15.2cm	0-3%	51.3%	492/386	Mansker series, calcareous, shallow brown colored soils	Native, perennial shrub in flower, slender stems yellow radiating heads
Grasses*	76.2cm	30.4cm	0-3%	73.3%	531/464	Brownfield series, deep, noncalcareous permeable, sandy soils	Clumps of green and brown grasses with spikelets

*Perennial threeawns (Aristida pansa), Sand dropseed (Sporobulus cryptandrus), Little bluestem (Schizachyrium scoparium), Sand bluestem (Androgogen hallii), Hairy gramma (Bouteloua hirsuta)
**Total biomass in grams/0.25 m^2

Table 3.2 Background information to the selected study sites.

	Latitude	Longitude	Annual rainfall	Average annual temperature
Creosote	$31^0$29'N	$103^0$5'W	28.1cm	25.5^0C
Broom snakeweed	$33^0$13'N	$102^0$50'W	40.6cm	16.1^0C
Shinnery oak	$33^0$25'N	$102^0$50'W	43.1cm	13.8^0C
Rough coldenia	$31^0$30'N	$103^0$08'W	28.1cm	25.5^0C
Grasses	$33^0$20'N	$102^0$50'W	40.6cm	16.1^0C

3.2.2 Vegetation Sampling Sites in the Southern High Plains

The shinnery oak (Quercus havardii), broom snakeweed (Xanthocephalum sarathrae) and mixed grass (Aristida pansa, Sporobolus cryptandrus, Schizachyrium scoparium, Andropogen hallii and Bouteloua hirsuta) sites all occur in the southern high plains zone of north Texas which also extends into eastern New Mexico and Oklahoma. Grasses predominate but forbs and woody plants have invaded areas of heavy grazing which is apparent at the sampling sites.

Sandy lands common throughout the region are dominated by shinnery oak. Shinnery oak occurs as climax vegetation spreading rapidly as grass vegetation disappears with overgrazing. Broom snakeweed, like shinnery oak and creosote bush, is an indicator of overgrazed grasslands but occupies a different soil type. The grass site occupies a sandy land range site of nearly level to gently sloping plains. The grass site, treated to control the spread of shinnery oak, is representative of a healthy grassland environment.

3.3 Data Collection

Bidirectional radiance measurements collected by the PARABOLA and support measurements were taken during a 10-day period in September, 1984. On September 11, 1984 an air-reconnaisance flight located the shinnery oak, oak/grass, grass and broom snakeweed sites to be sampled in the southern high plains vegetation zone. From September 12-14, the shinnery oak, grass and broomsnakeweed sites were sampled one day each. On-site field sampling included collection of PARABOLA data, sun photometer measurements ,photography and biomass estimates. The sampling procedure was repeated September 17-19 for the creosote and rough coldenia sites with limited collection for the mesquite and oak/grass sites due to time restrictions. Due to the similarities in sampling procedures throughout the study the procedure for only one day is outlined in the following discussion.

3.3.1 PARABOLA Data Collection

Prior to the actual sampling procedure a sampling timetable was determined to represent adequately solar

zenith angles found throughout the day. The sampling procedure started at approximately 9:00 am to represent a large solar zenith angle in order to collect a representative sampling of the full range of solar zenith angles.

Within each solar zenith angle collection period, five samples were taken, within a eleven minute period. To begin the sampling procedure, the TPMS was stationed at the selected starting point within the sampling field. The vehicle was placed facing directly into the sun aligned along the principle plane.

Once the vehicle was in position, four other sampling locations were marked one meter apart. At each sample location the PARABOLA collected data twice to insure against momentary instrument malfunction. The camera with fish-eye lens mounted adjacent to the sensor simulteanously photographed the ground conditions sampled by the PARABOLA. The camera on the TPMS was tripped manually to document sky conditions. This procedure, lasting approximately two minutes, was then repeated for four more sampling sites as the TPMS was moved forward to each sample plot location. At the end of five samples ,

the TPMS was returned to the original starting point for sampling in the next solar zenith angle. This procedure was repeated until each solar zenith angle selected was sampled.

There was approximately a 20 minute period between each solar zenith angle sampling. During this time, sun photometer measurements were collected. This procedure is described in detail in an ensuing section dealing with calibration.

Upon completion of data sampling, vegetation clippings were made randomly at the site to estimate biomass. Five 0.25 x 0.25 meter areas were clipped and sorted into dead and live vegetation. These vegetation samples were placed in bags and were then weighed before drying. Wet and dry biomass estimates were determined by a ratio of vegetation (grams) to the sampled area (0.25m squared), the results being tabulated in Table 3.1.

3.4 Calculation of Reflectance

3.4.1 Calibration of Spectral Radiance

An important aspect of the field spectral measurements relates to the calibration of the data. Field data show gains or offsets, thus, it is necessary to calibrate the instrument. Gain is defined as an increase in signal power in transmission from one point to another while an offset is the relation between a fixed reference point on an input scale and corresponding point on an output scale which must be known. Calibration implies comparison with measurements of a fixed energy source or standard reflectance instrument. A 182.8 cm intergrating sphere was the standard used for calibration in the laboratory. The intergrating sphere with multiple diffuse reflectors transfors output such that a 25.4 cm diameter exit window is filled with light uniformly. The PARABOLA is calibrated by creating a linear relationship between known values of radiance output and measurements of the intergrating sphere taken by the PARABOLA. Recent calibration shows the relationship between the recorded voltage and radiance is linear in all three spectral channels with a coefficient of determination (R^2) of 0.999 (Deering and Leone, 1984).

3.4.2 Calculation of Irradiance

To obtain reflectance, accurate measurement of irradiance is needed. There are several methods of measuring irradiance, the most common being to measure reflectance off a $BaSO_4$ panel which is assumed to be a perfect lambertian reflector. However, physical restrictions of the PARABOLA made barium sulfate readings impossible. To take readings the PARABOLA would have to been repeatedly lowered and raised throughout the sampling procedure which would have made the sampling process difficult, if not impossible.

An alternative strategy was to use a simple solar spectral model by Bird (1984), that was designed for application on cloudless days. The solar spectral model was modified by Eck (1985) of NASA/Goddard to calculate irradiance data with the input of sun photometer measurements. The modified model separately calculates direct and diffuse radiation as defined below:

Diffuse Horizontal Irradiance

$$Is\lambda = (Ir\lambda + Ia\lambda)C\lambda + Ig\lambda$$

Where:

$C\lambda$ = correction factor tabulated by Bird (1984)

$Ir\lambda$ = rayleigh scattered irradiance

Where:

$$Ir\lambda = Ho\lambda \cos(Z)\ TO\lambda\ Tw\lambda\ Tr\lambda\ (1-Ta\lambda)\ Wo\ Fa$$

Where:

Wo = single scattering albedo of the aerosol

Fa = is the forward to total scattering ratio of the aerosol*

* Bird (1984) suggests a value of 0.928 for the aerosol albedo and the value of Fa =0.82

$$Ig\lambda = [Id\lambda \cos(Z) + (Ir\lambda + Ia\lambda)\ C\lambda]pgPs/(1-PgPs)$$

Where:

Pg = ground albedo 0.5(red) and 0.4(NIR)

Ps = air albedo and is given by:

$$Ps = To'\lambda Tw'\lambda\ [Ta\lambda(1-Tr'\lambda)0.5 + Tr'\lambda(1-Ta'\lambda)0.22Wo]$$

The primes on the transmittance terms indicate that they are evaluated at an air mass of 1.9.

Direct Normal Irradiance

$Id\lambda = Ho\lambda Tr\lambda Ta\lambda To\lambda Tw\lambda$

Where:

$Ho\lambda$ = extraterrestrial spectral irradiance tabulated in Bird (1984)

$To\lambda$ = ozone absorption and is defined as:

$To\lambda = \exp(-Ao\lambda 0.344Mo)$

Where:

$Ao\lambda$ = Ozone absorption coefficient as tabulated in Bird (1984)

Mo = air mass expression for ozone

Where:

$Mo = 35.0/[1224.0 \cos^2(Z)+1]^{0.5}$

$Tw\lambda$ = water vapor absorption

Where:

$Tw\lambda = \{\exp 3.3285 Aw\lambda [W+(1.42-W)0.50]M/(1.0+20.7Aw\lambda M^{0.45}\}$

$Aw\lambda$ = water vapor absorption coefficient and is tabulated by Bird (1984)

W = precipitable water in a vertical path as tabulated from radiosonde data provided by the National Climatic Center

$Tr\lambda$ = rayleigh scattering transmittance function and is defined as:

$Tr\lambda = \exp\{-M'/[4(115.6406-1.335/\lambda^2)]\}$

Where:

$M = \cos(Z)+0.15(93.885-Z)^{-1.253}$

Z = apparent solar zenith angle

M' = pressure corrected air mass

Where:

$M' = MP/Po$

$Po = 1013mb$

P = is the measured surface pressure in mb

$Ta\lambda$ = aerosol extinction

$Ta\lambda$ = 1/m ln Ho voltage/sun photometer voltage$-(To\lambda+Tr\lambda)$

Comparison with corrected BaSO4 data collected on two separate dates in a 1983 PARABOLA experiment, show the modified model averages 1.5 percent accuracy in the red spectral region and 1.7 percent in the NIR (Table 3.3).

3.4.3 Sun Photometer Input to the Model

A major modification of the Bird (1984) model is the input of sun photometer measurements to calculate direct and diffuse irradiance. The sun photometer measures intensity of direct solar radiation in narrow wavelength bands. The atmospheric turbidity can be determined from the spectral measurements of direct solar radiation. The atmospheric turbidity is defined as the extinction of direct solar radiation by existing aerosols and is a major parameter in calculation of irradiance.

In practice the sun photometer is similar to a photographic exposure meter with a narrow viewing angle. Filters mounted on a disc within the hand-held instrument are rotated so that different filters (0.500um and 0.875um for this experiment) can be viewed through a glass plate. Measurements are taken separately for each filter by

Table 3.3 Comparison of solar irradiance derived from reflectances over BaSO4 and the Bird Spectral Model.

a)		8/3/83			8/10/83	
Time	7:35am	8:40am	9:38am	9:32am	10:34am	11:56am
Solar zenith	75.1	62.5	51.3	53.4	41.5	28.9
Corrected $BaSO_4$	7.26	16.38	23.76	26.1	32.41	39.09
Spectral model	7.22	16.30	23.87	24.48	31.91	38.73
Percent difference	0.6	0.5	-0.5	6.2	1.5	0.9

b)		8/3/83			8/10/83	
Time	7:35am	8:40am	9:38am	9:32am	10:34am	11:56am
Solar zenith	75.1	62.5	51.3	53.4	41.5	28.9
Corrected $BaSO_4$	4.44	10.13	14.95	16.22	20.5	24.8
Spectral model	4.11	10.02	14.76	15.86	20.68	24.96
Percent difference	7.4	1.1	1.1	2.2	-0.9	-0.6

aiming the instrument at the sun so that the direct solar beam falls on the target and the voltage output of the silicon detector is read by a device.

3.4.4 Calculation of Reflectance

A software program was developed by Eck(1983) at NASA/Goddard to calculate reflectance for PARABOLA data. With minor modifications, this program is used for the PARABOLA data collected in September, 1984. Modification to the program enables the introduction of the Bird(1984) model to calculate irradiance instead of calibrated BaSO4 readings.

Sun photometer readings are input into the Bird model to calculate irradiance for the the specific solar zenith angles at the time of collection. A linear fit is calculated and the program calculates the irradiance for any solar zenith angle. The program reads the calibrated PARABOLA data for one scan, calculates the irradiance for that solar zenith angle and simply calculates the reflectance.

3.5 Statistical Analysis

3.5.1 Transformed Divergence

Discrimination of surface types is dependent on a measurement of distance or separability between probability densities characterizing pattern classes (Swain and King, 1973). The level of statistical separability can be computed from the mean vectors and covariance matrices associated with each class by employing one of several statistical distance measures (Latty and Hoffer,1981). Divergence, while measuring statistical distance between pairs of classes, provides information on the separability of these classes. The separability of classes represents an estimate of the probability of correct classification for measurements provided (Latty and Hoffer,1981). In remote sensing, classes are assumed to have normal probability density functions, thus divergence is written as an expression involving means and covariance matrices (Swain and Davis, 1978). However, since divergence increases without bound as the statistical distance between classes increases, a saturation transform called transformed divergence was attempted which corresponds more closely with percent correct classification.

Transformed divergence programmed on NASA's IDIMS System was used to calculate separability between pairs of vegetation types based on their bidirectional reflectance data. Analysis of preliminary results showed that because of limited estimates of variance from the data that most were completely separable. Thus transformed divergence was found to be an inappropriate statistical test. These preliminary results are given in Appendix 1. The sensitivity of transformed divergence to these data is due to the wide separability between class means. This led to saturated values at most view angles and the small sample size (5) resulted in extremely small covariance values. The limitations cited above led to a re-evaluation of the statistical analysis used. As a result, the statistical test, student t, and a measure of dissimilarity, Euclidean distance were selected. A detailed discussion of the t-test and Euclidean distance follows.

3.5.2 Student's T-Test

The student's-t test is a small sample test for estimating and testing hypotheses about population means (Mendenhall, 1971). For the purposes of this research the

t-test is used to make inferences concerning the differences between two means that represent vegetation covers at specific view angles. The formula for the t-test is:

$$t = \frac{(\bar{y}_1 - \bar{y}_2)}{s\sqrt{\frac{1}{n_i} + \frac{1}{n_2}}}$$

Where:

y_1 = sample mean

y_2 = sample mean

n = number of samples

s = estimate of the population standard deviation

$$s = \frac{(n_1 - 1)s_1^2 + (n_2 - 1)s_2^2}{n_1 + n_2 - 2}$$

Where:

n+n-2 = number of degrees of freedom

s_1^2 = sample variance

s_2^2 = sample variance

The student's-t test is similar to the z-test whose probability distribution is the standardized normal distribution. the t-test, like the z-test is symmetrical about t=0, but unlike a normal distribution, it is much

more variable (Mendenhall, 1971). This variability is due to the randomness of the mean and variance which are independent of each other.

The null hypothesis for the difference between two means is that both samples are drawn from the same population. To test the hypothesis, the computed t-score is compared to the tabulated t-score. If the value of the calculated t is larger, then the null hypothesis is rejected, meaning the samples probably come from different populations with different means.

The t-test for the differences between two means is based upon two assumptions: (1) that the populations from which the samples are drawn are normally distributed , and (2) population variances are homogeneous. Although both assumptions can be violated with little effect on the conclusions drawn from the t-test (Thorne, 1980), a test for homogeneity of variance was made prior to computation of the t-test. A description of the test and results are found in Section 3.5.3.

Three objectives were achieved by using the t-test in analzing the differences between means:

1. to test differences between vegetation covers,
2. to test view angle differences within vegetation covers and
3. to test solar zenith angle differences within vegetation covers.

The first objective was to test the significance of differences of the means between vegetation covers at nadir. T-values for each solar zenith angle in the visible and NIR were calculated. Vegetation that showed insignificant differences between the means at nadir were then tested at all view angles to indicate changing values between classes with off-nadir viewing, thus suggesting a possible increase in information content.

In addition to the t-test for significance between the class pairs, variability within classes was tested for view angle and solar zenith angle changes. Within each of the solar zenith angle per class, differences between nadir and off-nadir view angle means were calculated for the visible and NIR reflectance measurements. Thus, for each class having five solar zenith angles, ten calculations were made. Solar zenith angle variability was calculated by comparing identical view angles from

each of the solar zenith angles within every vegetation cover type.

3.5.3 F-Test for Equal Variance

As previously mentioned, tests for equal variance of means is often calculated prior to performing the t-test to assess the assumption of equal variances. The F-test, a small sample statistical method, compares two population variances using the ratio of the sample variances (S2/S1). Independently drawn samples from normal distributions with equal variances possess a probability distribution in repeated sampling known as an F distribution. The F distribution is nonsymmetrical and depends upon the number of degrees of freedom associated with each sample variance. To test the null hypothesis , the critical value found in the F tables is compared to the calculated F from the variance ratio. If the calculated F is greater than the critical F at the 1 percent level then the null hypothesis is rejected, suggesting the samples are drawn from different populations.

The F-test was performed on the data for testing both

equal variance within and between classes. Prior to calculating the means test, the F-test for the following combinations was performed:

1. Within class mean nadir value vs. every other view angle within a solar zenith angle,
2. Between each class pair mean for every view angle, and
3. Within class between solar zenith angles.

The F-test for equal variance within canopies indicated that 98.6 percent of differences between off-nadir and nadir were insignificant, while 98.4 percent of the differences in solar zenith angles were found to be insignificant. In addition, 97.9 percent of the class pairs showed variances between the reflectance values were equal.

3.6 Euclidean Distance

The most common measure of dissimilarity, Euclidean distance, is used as a measure of statisitical separability between classes computed for all class pairs. The degree of dissimilarity between classes is provided

simply by the distance between the class means, defined by the rectangular coordinate system. Thus the larger the Euclidean distance, the greater the statistical distance and higher probability of correct classification (Kieffer and Lillisand, 1979). The Euclidean distance equation in n-dimensional space is defined as:

$$D_{ab} = [^{i=p} (X_{ia}-X_{ib})^2]^{1/2}$$

Where:

$i = 1,2, \ldots,P$

P = total number of axes

X_{ia} = the projection of sample a on the ith axis

x_{ib} = the projection of sample b on the ith axis

The resulting Euclidean distance coefficient is a measure of dissimilarity ranging from zero (similarily) to positive infinity.

One-dimensional Euclidean distances are calculated separatedly for the NIR and visible wavelengths between class pairs for each view angle. In addition, Euclidean distance for the NIR and visible between class pairs is calculated. These combinations are expected to indicate which wavelength may be responsible for adding greatest separability between class pairs. In addition to the above combinations, selected multiple combinations of view angles between 45 degrees in the backscatter to 45 degrees in the forward scatter were calculated. The combinations are limited to within 45 degrees view angles in the bidirectional reflectance distribution for two reasons: the extreme variability found with different solar zentih angles beyond 45 degrees and the atmospheric effects existing at these larger view angles that would limit use in any classification algorithm.

4 RESULTS

An evaluation of the bidirectional reflectance distribution of each canopy is the first step in analyzing the results. The data are representative of plant canopies ranging from almost bare soil to complete canopy cover. Observations for the principle plane are first provided for:

1. complete vegetation canopies,
2. bare soil,
3. sparse vegetation canopies, and
4. impact of shadowing on bidirectional reflectance of canopies.

The general characteristics discussed in each of these categories may be expected to account for most of the trends found in bidirectional reflectance distributions of plant canopies. However, other factors affect the bidirectional reflectance characteristics, for example, leaf angle orientation, has a marked influence on bidirectional reflectance. Each plant cover analysis includes a separate discussion of the bidirectional reflectance distributions in the red and NIR spectral

regions. Using the t-test, differences in reflectances were compared for the following conditions: 1) to compare off-nadir view angles and nadir in the backscatter and forward scatter direction, and 2) to compare solar zenith angles at every view angle.

4.1 Complete Vegetation Canopy Bidirectional Reflectance

Anisotropic scattering of vegetation canopies generally results in increasing reflectance with off-nadir view angles for all solar zenith angles. The peak reflectance occurs in the direction of the sun referred to as the backscatter direction. This trend occurs for both the red and NIR bands with the magnitude of reflectance greater in the NIR. These trends have been shown by Kimes (1984) and are clearly illustrated in Figs. 4.1-4.5. Kimes (1984) suggests increasing reflectance with off-nadir viewing is a function of viewing different proportions of the canopy layers as the view angle changes. As the view angle increases a higher percentage of upper canopy layers are viewed. The proportion of shadowed canopy to sunlit canopy layers increases with depth into the canopy structure. Thus, viewing a higher percentage of upper canopy layers results in higher reflectances. Increasing solar zenith angles are also

a)

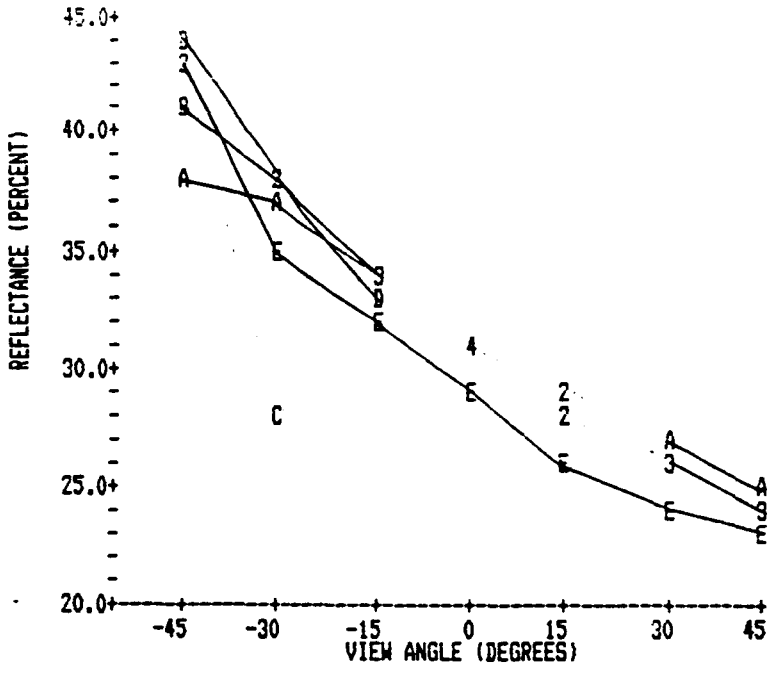

b)

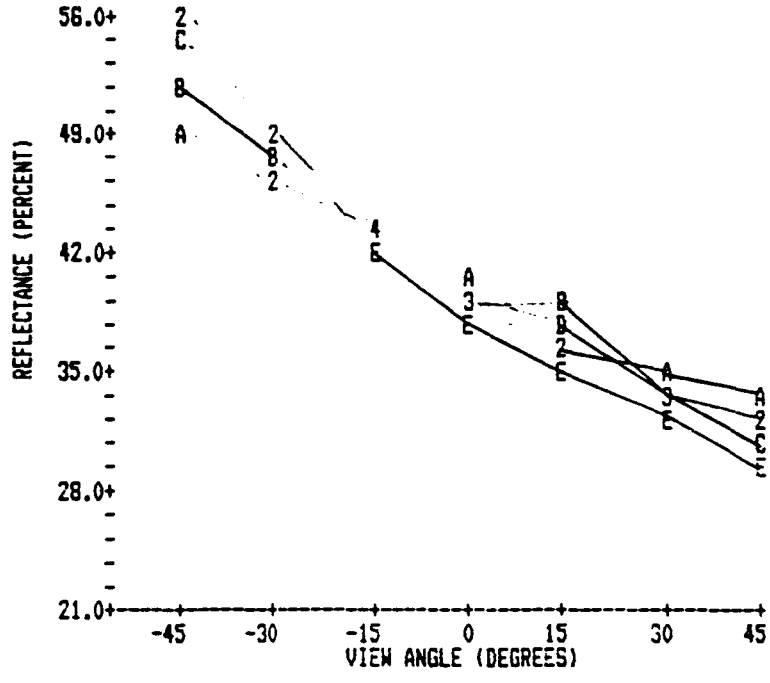

4.1 Change in reflectance with view angle for 5 solar zenith angles (A=30^0,B=38^0,C=45^0,D=54^0 and E=60^0), for the a) red and b) NIR spectral bands for the rough coldenia canopy.

a)

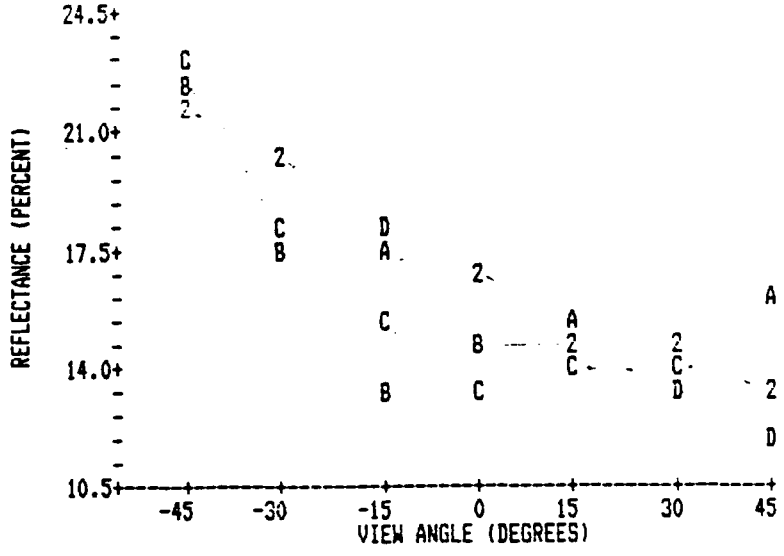

b)

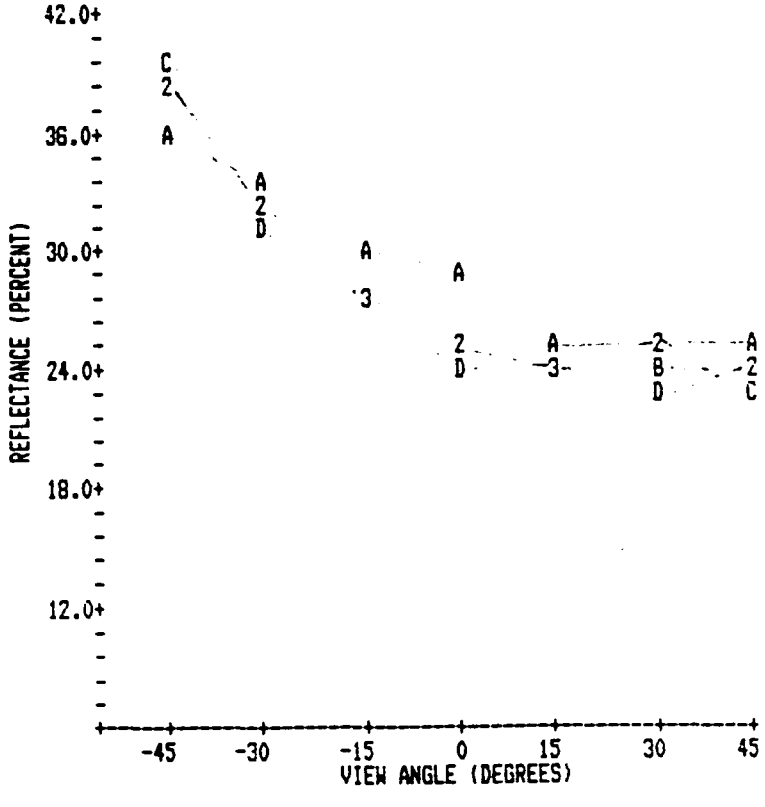

4.2 Change in reflectance with view angle for 4 solar zenith angles (A=30 ^{0},B=45 ^{0},C=54 ^{0},D=60 ^{0}), for the a) red and b) NIR spectral bands for the creosote canopy.

a)

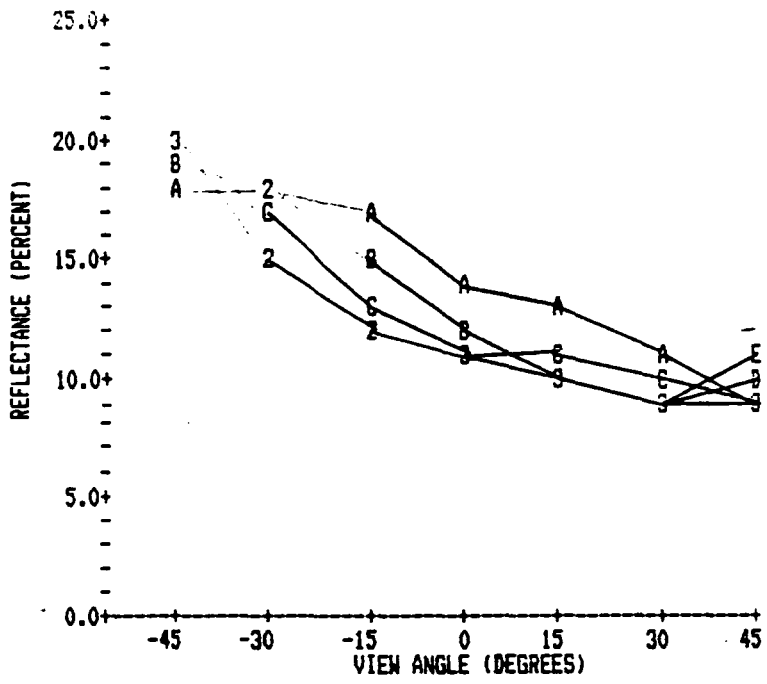

b)

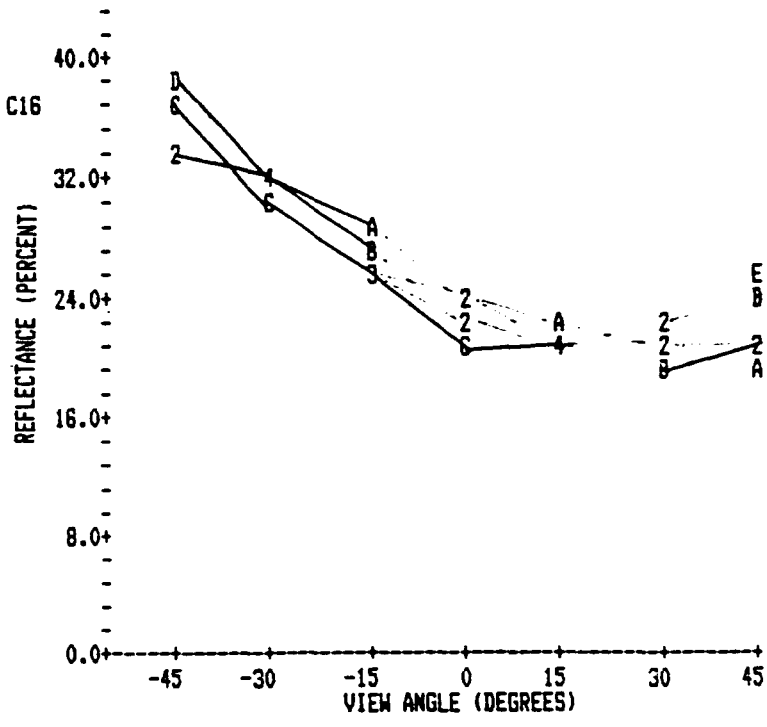

4.3 Change in reflectance with view angle for 5 solar zenith angles ($A=30^0, B=38^0, C=45^0, D=54^0, E=60^0$), for the a) red and b) NIR spectral bands for the grass canopy.

a)

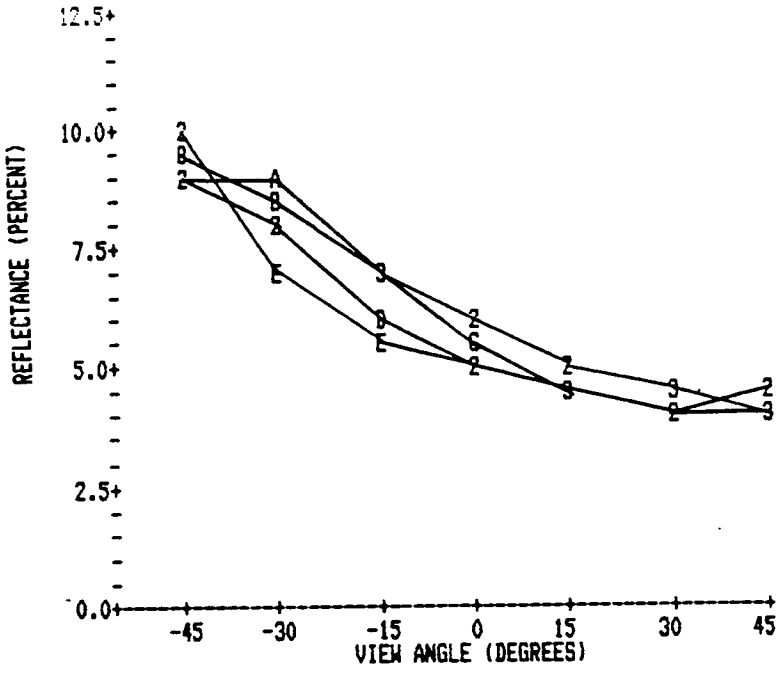

b)

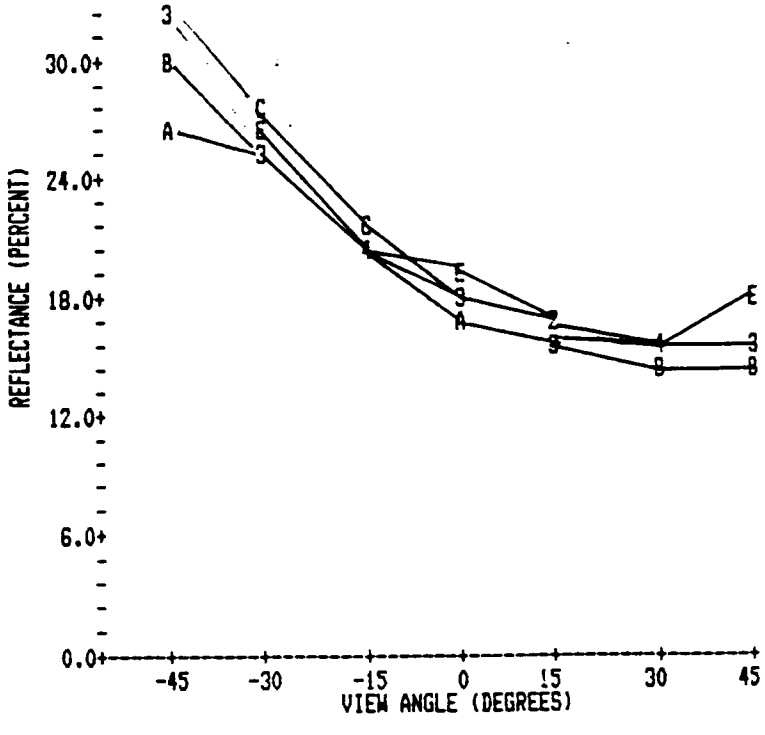

4.4 Change in reflectance with view angle for 5 solar zenith angles (A=30^0,B=38^0,C=45^0,D=54^0,E=60^0), for the a) red and b) NIR spectral bands for the shinnery oak canopy.

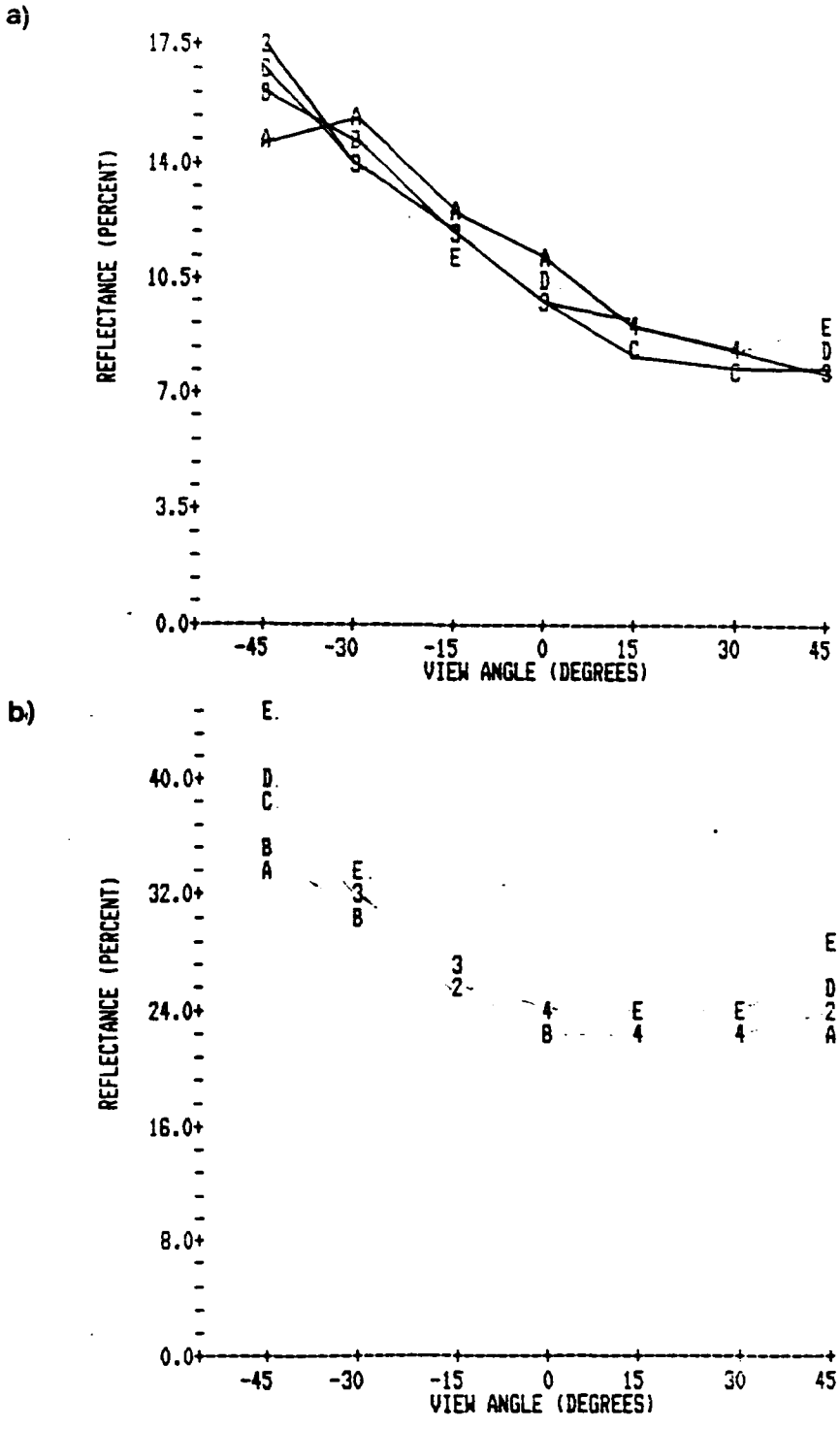

4.5 Change in reflectance with view angle for 5 solar zenith angles (A=30^0,B=38^0,C=45^0,D=54^0,E=60^0), for the a) red and b) NIR spectral bands for the snakeweed canopy.

reported to increase reflectance at larger view angles by illuminating a greater percentage of upper canopy layers (Kimes, 1983).

Results presented in Figs. 4.1-4.5 show red and NIR reflectances are generally higher in the backscatter than forward scatter direction. Although the sensor is viewing a higher proportion of upper plant canopy components with increasing view angle, increased shadowing is also observed in the forward scatter direction. Kimes (1984) suggests that the interaction of these two mechanisms result in the minimum reflectance off-nadir in the forward scattering direction.

Results presented in Figs. 4.1-4.5 illustrate that reflectance in the NIR is more symmetric around nadir than the red spectral region. This can be explained by the scattering properties inherent in NIR reflectance. In addition to the mechanisms previously described, NIR reflectance also increases with off-nadir angles due to viewing increasing multiple layering of leaves. It has been shown that additive reflectance occurs due to the transmittance and reflectance properties of the NIR (Swain and Davis, 1978). The fifty percent reflectance and

transmittance properties typical of most leaves (Swain and Davis, 1978), results in illumination of lower canopy layers that reflect back through the upper canopies thus increasing reflectance.

4.1.1 Anisotropic Scattering Properties of Soil

The bidirectional reflectance of soils shows strong anisotropic scattering properties with off-nadir viewing (Kirchner,1981). Reflectance is known to increase with increasing off-nadir viewing in the backscatter direction and to decrease to a minimum reflectance in the forward scatter direction. The largest variations in bidirectional reflectance appear to occur at large solar zenith angles. These trends are well documented in the literature (Kimes,1983, Kirchner,1982) and it is argued that the opaque nature of soils, that results in low transmittance, is responsible. Rough coldenia's very low plant density (16.4 percent) results in characteristics similar to that of bare soil. This can be seen in Fig. 4.1. A strong backscatter occurs because only surfaces in direct sunlight are viewed by the sensor. As the sensor moves to the anti-solar direction, Kimes (1984) suggests

that the contribution of shadows caused by the opaque components increases.

4.1.2 Sparse Canopy Bidirectional Reflectance

In sparse canopies, the scattering properties of vegetation and soil combine to form a unique reflectance distribution. A comparison of shinnery oak (plant density 48.5 percent) and grass (73.3 percent) with rough coldenia (plant density 18.4 percent) shows that sparser canopies exhibit a stronger backscatter than more complete vegetation canopies. In addition, the minimum reflectance occurring at larger forward scatter view angles in a sparser canopy is illustrated by the the rough coldenia (Fig. 4.1).

Kimes (1984) suggests the variability of bidirectional reflectance in a sparse canopy is greatest at small solar zenith angles due to the higher soil contribution. As the solar zenith angles increase, variability decreases because less soil and more vegetation is being viewed, thus, the bidirectional reflectance properties resemble a more complete vegetation

canopy. From an examination of Figs.4.1-4.5 this trend is clearly illustrated.

4.1.3 Impact of Shadowing on Bidirectional Reflectance of Plant Canopies

Shadowing is a significant factor in the bidirectional reflectance of a plant canopy. The amount of shadow seen is a function of solar zenith and view angle. For example, Appendix 2 indicates that the shadowed proportion of all the vegetation cover types vary with solar zenith and view angles. The shadowing results (Appendix 2) illustrate two trends: 1) shadowing increases from the forward to backscatter direction and 2) shadowing increases with increasing solar zenith angle increases at every view angle. Also evident is the differences in magnitude of shadowing among the vegetation covers. This characteristic depends primarily on the plant density and transmittance properties of a canopy. For example, the effect of opaque components of vegetation canopies and bare soil are significant since transmittance properties are zero.

The effect of opaque materials on shadowing is clearly shown in examining the shinnery oak and grass canopies. Although the grass canopy has a substantially higher plant density than the shinnery oak, the latter exhibits a greater overall shadowing effect. This is likely due to the shinnery oak being a woody plant with a high percentage of opaque material, where as the grass canopy has higher transmittance properties than the shinnery oak canopy. Another example is shown by examining the shinnery oak and snakeweed canopies. Both canopies have approximately the same plant density, however, the shadowing effect is much more pronounced in the shinnery oak. This also may be explained by the greater amount of woody biomass exhibited by the shinnery oak.

An attempt was made to correlate NIR and red reflectance values with percent shadow in the forward and backscatter direction of each vegetation canopy. Reflectances in the backscatter and forward scatter direction for every solar zenith angle were first correlated separately against percent shadow. In the forward scatter direction the correlation coefficient between reflectance and shadowing for the rough coldenia

was -.51 (red) and .47 (NIR), while, the correlation coefficient for the other canopies were all below .28. Since rough coldenia has a sparse canopy cover, reflectance values are dominated by the large soil area viewed and to a lesser extent by the canopy characteristics. Shadowing on the soil surface would thus have a direct impact on reflectance values on the forward scatter direction. However, in the denser canopies the diversity of canopy characteristics affecting reflectance may mask the impact shadow has on the reflectance values.

Strong negative correlations between NIR and red reflectance and shadowing occurred in the backscatter direction for the plant canopies except the rough coldenia. The highest correlation coefficient between shadowing and reflectance in the backscatter direction occurs in the shinnery oak canopy ($r = -.77$ (red), $r = -.63$ (NIR)). However, the other canopies all had relatively strong correlations as well. For example, the grass and snakeweed canopies had strong similar correlation coefficients. The grass had a correlation coefficient of -.66 in the red and -.43 in the NIR, while the snakeweed had correlations of -.66 in the red and -.49 in the NIR. These correlation coefficients indicate that

relationships between reflectance and shadowing were stronger in the red spectral region. The more pronounced effect of shadowing in the red spectral region also has been referred to by Colwell (1974) and attributed to lower transmittance properties found in the red spectral region.

4.1.4 Rough Coldenia Canopy Bidirectional Reflectance

The bidirectional reflectance pattern of rough coldenia, illustrated in Fig. 4.1, is similar to that of bare soil in both the NIR and red spectral bands. Since plant density is 18.4 percent, this observation may be attributed to the anisotropic properties of soils dominating the reflectance patterns. Fig. 4.1 shows reflectances increase linearly as off-nadir view angles increase in the backscatter direction. Reflectances decrease linearly with increasing off-nadir angles in the forward scatter direction. However, at larger solar zenith angles the effect of soil is less pronounced with vegetation scattering properties begining to dominate the bidirectional reflectance pattern. The results given in Fig. 4.1 are consistent with the findings of Kimes (1984) in that the influence of soil scattering properties is at a maximum at the small solar zenith angles. Kimes (1984)

suggests that this is due to soil illumination being the highest with smallest solar zenith angles in a plant canopy.

Significant differences in reflectance, tested using student's t-test, between nadir and most off-nadir view angles are found for the NIR and red spectral regions at all solar zenith angles. Significant differences in reflectance between solar zenith angles in both the red and NIR bands of the rough coldenia canopy are limited to the backscatter direction (Appendix 4). However, some differences in reflectance occur between the largest and smallest solar zenith angles in view angles other than those found in the backscatter direction. These significant differences in reflectances are slightly more pronounced in the NIR. This finding may also be explained by the bidirectional reflectance distribution changing from one being more characteristic of a bare soil (small solar zenith angle), to one resembling the bidirectional reflectance of a vegetation canopy at large solar zenith angles.

4.1.5 Creosote Bidirectional Reflectance

Soil scattering properties dominate the bidirectional reflectance of creosote for both the red and NIR spectral regions (Fig. 4.2). This is shown by the linear relationship between reflectance and view angle, shown in Fig. 4.2, that is typical of the bidirectional reflectance of a bare soil. With a low plant density (14.7 percent), the high red reflectance in the backscatter direction may be attributed to the significant scattering properties of soil observed at greater off-nadir angles. Small solar zenith angles show high reflectance values that are typical of a soil bidirectional reflectance distribution. As the solar zenith angles increase, the percentage of soil viewed by the sensor decreases and vegetation viewed increases, resulting in lower reflectance values in the backscatter direction (Fig. 4.2). Reflectance decreases in the forward scatter direction due to the greater properties of shadowed surface components that increase with increasing off-nadir angles.

Like the rough coldenia canopy, the relationship between reflectance and view angles in the red spectral

region is generally linear in the creosote canopy. However, the change in reflectance with increasing view angle in the backscatter, and decrease in reflectance with increasing view angle in the forward scatter direction is not as pronounced. Thus, the backscatter and forward scatter direction view angle reflectances show little or no significant differences from nadir in the red band. This finding may be caused by the relative height of the creosote canopy (213 cm) to the instrument (457 cm). At increasing off-nadir view angles the proportion of vegetation being viewed increases substantially with a taller canopy. The increased proportion of vegetation viewed masks the generally strong backscatter response of the bare soil.

Vegetation scattering properties are more apparent in the NIR bidirectional reflectance than in the red spectral region, although the underlying soil still dominates the characteristics of the reflectance curve (Fig. 4.2). As was found in the rough coldenia canopy, the influence of soil is most dominant at small solar zenith angles because the proportion of solar illumination is at a maximum. At these small solar zenith angles the relationship between reflectance and view angles is nearly linear. As the

solar zenith angle increases, the bidirectional reflectance distribution resembles a sparse canopy because less soil is viewed by the sensor and the proportion of upper canopy layers viewed increases. Reflectance also increases at larger solar zenith angles due to the effect of multiple layers of vegetation that increases reflectance in the NIR. This trend has also been shown for the rough coldenia canopy and is clearly illustrated in Fig. 4.2.

Significant differences in reflectances do exist between most backscatter view angles and nadir in the NIR band of the creosote canopy (Appendix 3). Although, the backscatter direction of creosote in the red and NIR have similar reflectance trends, the high variability associated with the red spectral region of the creosote is not as pronounced in the NIR.

4.1.6 Grass Canopy Bidirectional Reflectance

The red spectral region of the grass canopy (erectophile) shows continuously decreasing reflectance from 45 degrees in the backscatter to a minimum

reflectance in the forward scatter direction (Fig. 4.3). The minimum reflectance found at the large off-nadir angles occurs with smaller solar zenith angles and approaches nadir as the solar zenith angle increases. The relatively high plant density (50.0 percent) of the grass canopy limits the influence of bare soil to the smallest solar zenith angles. At the smaller solar zenith angles greater solar illumination of the bare soil results in higher overall bidirectional reflectance than larger solar zenith angles. The bidirectional reflectance of the grass canopy resembles a more complete vegetation canopy at larger solar zenith angles.

The differences in reflectance between off-nadir view angles and nadir in the red spectral region for the grass canopy are generally more pronounced in the backscatter direction. This trend is found for all solar zenith angles and may be explained by the scattering properties of complete vegetation canopies that are known to increase reflectance in the backscatter direction with increasing off-nadir view angles and increasing solar zenith angles.

The decrease of significant differences in reflectance between nadir and off-nadir view angles with

increasing solar zenith angles in the forward scatter direction results from the minimum reflectance shifting closer to nadir with increasing solar zenith angle. The forward scatter bidirectional reflectance distribution in the red spectral region may be explained by the significant amount of shadowing resulting from high plant density, decreasing percent soil being viewed and increase in percent of low reflecting vegetation being viewed. While these mechanisms usually lower reflectance in the forward scatter direction, at the larger view angles in the higher solar zenith angles, the effect of upper canopy components and possible specular reflectance viewed, causes reflectance to increase.

Most of the variability in reflectance with solar zenith angle changes in the grass canopy red spectral region occurs within 30 degrees in the forward and backscatter direction between the higher and smallest solar zenith angles. This pattern is attributed to the following trends:

1. smaller solar zenith angle bidirectional reflectances resemble those of a bare soil, and
2. larger solar zenith angle bidirectional reflectances resemble those of a complete vegetation canopy.

Results presented in Fig. 4.3 show the NIR grass canopy bidirectional reflectance distribution decreases from 45 degrees in the backscatter direction to a minimum reflectance in the forward scatter direction. The minimum reflectance is found at larger view angles in the smaller solar zenith angles. As solar zenith angles increase, minimum reflectance approaches nadir. This trend is identical to that found in the red spectral region, however, the magnitude of reflectance values is substantially different. The anisotropic properties of soil do not have a pronounced affect on the NIR grass canopy reflectance. Fig. 4.3 clearly illustrates that, unlike the red spectral region, the influence of bare soil is limited to the smallest solar zenith angle. As the solar zenith angle increases, bidirectional reflectance in the forward scatter direction is similar to that found in a more complete vegetation canopy.

Significant differences in reflectance with solar zenith angle variability in the NIR grass canopy reflectance occur at 45 degrees view angle in the backscatter and forward scatter direction. This trend may be attributed to the increased vegetation scattering properties that results in highest reflectance at large

view angles.

4.1.7 Snakeweed Canopy Bidirectional Reflectance

The red band bidirectional reflectance distribution of snakeweed (Fig. 4.4) shows maximum reflectance in the backscatter direction with reflectances decreasing to a minimum reflectance in the larger off-nadir view angles in the forward scatter direction. The influence of vegetation scattering mechanisms is likely to be responsible for the strong backscatter peak. The soil background has little effect on reflectance due to the high plant density (50.0 percent). The strong backscatter reflectance accounts for significant differences in reflectance from nadir being more pronounced in the backscatter direction than the forward scatter direction for all solar zenith angles (Appendix 3).

Variability in reflectance of snakeweed with changing solar zenith angles in the red spectral region only appears in the largest view angles for both the forward and backscatter direction. At 45 degrees view angle in the backscatter direction, the lowest reflectance values

occur at the smallest solar zenith angle (30 degrees). The remaining solar zenith angles have substantially higher reflectances. Thus, the reflectances at the smallest solar zenith angle are significantly different from reflectances in the remaining solar zenith angles. This trend may be attributed to the exponential increase in reflectance with increasing solar zenith angles, this being shown in the bidirectional reflectance distribution of snakeweed (Fig. 4.4).

The NIR backscatter bidirectional reflectance of snakeweed is dominated by the multiple layering of the canopy and increasing proportion of upper canopy layers that are viewed with increasing off-nadir angles. The reflectance in the forward scatter direction behaves similarly to that of the backscatter direction but with reduced reflectance values.

An examination of the red bidirectional reflectance distribution (Fig. 4.4a) with the NIR in Fig. 4.4b shows that for all solar zenith angles the minimum reflectance in the NIR occurs closer to nadir than that of the red spectral region. This illustrates the substantially lesser influence of bare soil in the NIR compared to the

red spectral region. In addition, the substantially higher reflectance with increasing solar zenith angle and view angle is evident.

All view angles in the NIR backscatter direction of snakeweed have significantly different reflectances from nadir for all solar zenith angles, while only at 45 degrees in the large solar zenith angles in the forward scatter direction do significant differences in reflectance occur (Appendix 3). The minimum reflectance occurs at 15 degrees in the forward scatter direction for all solar zenith angles. Thus, significant differences in reflectances are unlikely to occur in the forward scatter direction except at large view angles for the larger solar solar zenith angles.

The forward scatter direction of the snakeweed NIR bidirectional reflectance distribution shows significant differences in reflectance between the largest and the smaller solar zenith angles for all view angles, in addition to significant differences at 45 degrees backscatter in most solar zenith angles. The bidirectional reflectance distribution of snakeweed shows reflectances between solar zenith angles are similar

between 15 degrees backscatter and nadir and diverge at larger view angles in both directions. Thus, the forward scatter direction shows greater varibility in reflectance with solar zenith angle changes.

4.1.8 Shinnery Oak Bidirectional Reflectance

Comparison of Figs. 4.4 and 4.5 illustrate the similarity of reflectance characteristics of shinnery oak to that of snakeweed in the red and NIR bidirectional reflectance distribution. The similarities may be explained by both canopies having spherical leaf orientations, and similar plant densities that result in comparable shadowing effects. The differences in magnitude of the red and NIR reflectance from the snakeweed canopy is probably due to the specific reflectance, transmittance and absorption characteristics of the individual plants.

Significant differences in reflectance between nadir and off-nadir view angles in the red and NIR distributions are similar to those found in the snakeweed and grass canopies. Significant differences in reflectance occur in

the red spectral region from nadir beyond 15 degrees view angle in both the forward and backscatter direction in the smaller solar zenith angles. As solar zenith angles increase, significant differences in reflectances between off-nadir and nadir decrease in the forward scatter direction while remaining constant in the backscatter direction.

In the NIR, significant differences in reflectance between off-nadir view angles and nadir are generally restricted to the backscatter direction for all solar zenith angles (Appendix 3). These trends are very similar to those found in the snakeweed and grass canopies and may be attributed to the general scattering properties of vegetation described previously.

Significant differences in reflectance occur between the largest solar zenith angle and other solar zenith angles in the backscatter direction except at 45 degrees view angle (Appendix 4). This finding may be explained by examining the bidirectional reflectance of shinnery oak which shows solar zenith angle bidirectional reflectances parallel each other from approximately 15 degrees forward scatter direction to 30 degrees in the backscatter

direction (Fig. 4.5). However, at 45 degrees, the reflectance values converge, resulting in insignificant differences between solar zenith angles. In the forward scatter direction, reflectance values diverge at larger view angles, resulting in significant differences between solar zenith angles.

An examination of the bidirectional reflectance distribution of shinnery oak in the backscatter direction in the NIR shows that the smallest solar zenith angles have significantly lower reflectance than the remaining solar zenith angles in the large off-nadir angles. Unlike the backscatter direction, the significant differences in reflectance between solar zenith angles in the forward scatter direction are explained by the largest solar zenith angles being most distant from smaller solar zenith angles in the larger off-nadir angles.

4.2 T-Test for Differences Between Vegetation Canopies

Within the NIR, grass, snakeweed and creosote have similar reflectances at nadir for all solar zenith angles as an examination of Figs. 4.1-4.5 indicates. Analysis of results from Appendix 5 illustrates insignificant differences between these species reflectances at nadir.

In addition, rough coldenia is shown to be significantly different from all the vegetation types at all solar zenith angles while shinnery oak only resembles grass in the middle solar zenith angles. The bidirectional reflectance distributions of shinnery oak and rough coldenia (Figs. 4.1 and 4.4) show why they are significantly different from each other and other vegetation types. For example, shinnery oak is shown to have low reflectance relative to the other vegetation types while the rough coldenia in comparison has the highest overall reflectance distribution.

Fewer vegetation cover pairs, shown in Appendix 5, are found to be similar at nadir in the red distribution. Again, the grass, snakeweed and creosote canopies show similar reflectance values at nadir. Appendix 5 shows shinnery oak and rough coldenia to be significantly different from all other cover types at every solar zenith angle.

Table 4.1 presents the solar zenith angle differences at all view angles for the vegetation pairs found not to differ at nadir. Analysis of the results for the red band combinations show that the forward scattering direction

Table 4.1 Students t-values for comparison for reflectances at selected view angles for canopy combinations which had indistinguishable reflectances at nadir. (Underlined t-values indicate significant differences at the 99 percent level).

			View angle						
Canopy combinations	Solar zenith angle	Channel	-45^0	-30^0	-15^0	0^0	$+15^0$	$+30^0$	$+45^0$
Grass-Creosote	30^0	1	2.6	3.0	.48	1.8	1.9	2.5	6.6
Grass-Snakeweed	30^0	2	.03	19.	1.3	.77	.80	1.7	6.2
Grass-Creosote	30^0	2	2.0	1.1	.73	2.0	1.2	3.8	10.
Grass-Snakeweed	38^0	1	3.4	3.3	2.4	2.7	2.5	3.2	6.2
Shinnery Oak-Grass	38^0	2	2.3	5.8	2.7	3.3	5.3	6.3	19.
Grass-Snakeweed	38^0	2	1.1	1.3	.68	.84	2.0	4.5	10.
Grass-Snakeweed	46^0	1	3.0	3.4	1.8	1.9	3.5	4.0	3.1
Grass-Creosote	46^0	1	1.2	.21	.14	1.8	2.6	4.5	3.0
Snakeweed-Creosote	46^0	1	4.8	2.9	.91	2.8	3.8	6.7	4.1
Snakeweed-Grass	46^0	2	2.4	1.7	1.8	1.2	2.4	4.6	10.
Shinnery oak-Creosote	46^0	2	4.9	2.6	3.3	3.5	5.0	5.6	7.3
Grass-Snakeweed	46^0	2	.81	.09	.82	1.8	.77	2.7	6.0
Grass-Creosote	46^0	2	1.0	.73	1.6	2.5	2.1	2.8	2.3
Snakeweed-Creosote	46^0	2	.63	1.0	1.4	1.6	2.2	1.5	1.0
Grass-Snakeweed	54^0	1	3.0	1.2	1.2	.64	1.9	1.6	7.4
Grass-Creosote	54^0	1	1.8	3.0	1.9	1.8	3.0	5.7	3.0
Snakeweed-Creosote	54^0	1	4.0	3.6	2.7	2.1	3.9	7.0	4.2
Shinnery oak-Grass	54^0	2	3.3	2.7	2.3	3.0	3.3	3.3	10.
Grass-Snakeweed	54^0	2	.36	.36	1.4	1.1	1.4	.84	5.2
Grass-Creosote	54^0	2	.58	.22	1.2	1.8	2.6	1.4	.04
Snakeweed-Creosote	54^0	2	.63	.24	.41	1.3	1.8	1.2	3.5
Grass-Snakeweed	63^0	1	3.3	3.4	1.1	1.7	1.3	2.3	6.0
Shinnery oak-Grass	63^0	2	6.1	2.7	1.9	3.2	2.3	4.7	7.5
Grass-Snakeweed	63^0	2	.54	.49	.93	.12	1.8	2.0	3.2
Grass-Creosote	63^0	2	1.6	.49	1.3	.02	1.6	.05	1.9
Snakeweed-Creosote	63^0	2	3.4	1.5	1.1	1.1	.02	2.2	5.5

C-2

generally provides larger differences than the backscatter direction. The grass-creosote combination shows significant differences at the larger off-nadir view angles in the forward scatter direction with small solar zenith angles, while the snakeweed-creosote pair shows significant differences for all forward scatter view angles and larger view angles in the backscatter. The grass-weed pair was shown to be significantly different in both the forward and backscatter direction with no particular advantage to either direction.

Significant differences in the NIR distribution were also found to be more pronounced in the forward scatter direction. The grass-weed combination was significantly different only at larger off-nadir angles in the forward scatter direction while grass-creosote showed no significant differences at any view angle except in the 30 degree solar zenith angle. The weed-creosote, oak-grass and oak-creosote pairs all showed significant differences in the forward scatter were slightly better than the backscatter direction.

4.3 Euclidean Distances Between Vegetation Canopies

Appendix 5 and Tables 4.2 and 4.3 present the results of Euclidean distances between the paired vegetation canopies. Based on these results the following trends were observed:

1. within the red spectral region the backscatter direction consistently has the highest Euclidean distances between vegetation canopies,
2. within the NIR spectral region the highest Euclidean distances between vegetation canopies occur in the forward scatter direction, and
3. the red spectral region shows consistently higher Euclidean distances between paired vegetation canopies than the NIR.

In the following analysis descriptions of each of these characteristics is discussed in detail.

4.3.1 Comparisons in the Backscatter Direction

The highest Euclidean distances found between vegetation canopies in the red spectral region occur in the backscatter direction. An examination of Appendix 5 also indicates that within the backscatter direction the highest value is generally found at 45 degrees. This

Table 4.2 Euclidean distances between reflectances of canopy pairs calculated using 3-dimensional feature space of canopy reflectances at view angles of -30^0,$-15^0$and nadir for red, NIR and percent difference between the red and NIR reflectances.

Canopy combinations	NIR (.81-.84um)					Red (.65-.67um)					Percent difference				
	Solar zenith angle														
	30^0	38^0	45^0	54^0	60^0	30^0	38^0	45^0	54^0	60^0	30^0	38^0	45^0	54^0	60^0
Shinnery oak-Grass	13.4	10.2	5.9	8.8	9.5	15.5	14.0	12.4	11.0	12.0	15.6	37.2	11.0	25.0	26.3
Shinnery oak-Rough coldenia	39.2	39.0	36.8	38.9	35.4	46.7	47.3	47.4	48.0	45.3	19.1	21.2	28.2	23.3	27.9
Shinnery oak-Snakeweed	11.5	9.1	7.8	10.8	11.0	9.7	8.7	8.6	9.9	10.0	18.5	4.5	10.2	-8.0	-10.
Shinnery oak-Creosote	16.9	-	10.7	11.8	10.6	18.7	-	14.2	16.1	21.6	10.0	-	34.5	39.8	103.
Grass-Rough coldenia	25.8	29.0	31.0	30.2	26.0	31.2	39.3	35.1	36.9	33.3	21.7	14.8	13.2	22.1	28.0
Grass-Snakeweed	2.1	1.8	2.5	2.3	1.9	5.8	5.3	3.9	1.1	2.0	176.	194.	56.0	-109	5.2
Grass-Creosote	4.0	-	5.4	3.6	2.8	3.5	-	3.0	5.1	9.6	-14.	-	-8.0	42.8	242.
Rough coldenia-Snakeweed	27.7	29.9	29.0	28.0	24.3	37.0	38.6	38.8	38.1	35.3	35.0	29.0	33.7	36.0	41.1
Rough coldenia-Creosote	22.4	-	26.2	27.1	24.9	28.0	-	33.5	31.8	23.9	25.0	-	27.8	15.1	-4.1
Snakeweed-Creosote	5.7	-	2.9	1.5	2.8	9.0	-	6.0	6.2	11.5	51.8	-	106.	246.	310.

Table 4.3 Euclidean distances between reflectances of canopy pairs calculated using 4-dimensional feature space of canopy reflectances at view angles of -45^0,-30^0,-15^0 and nadir for specified solar zenith angles for the red, NIR and percent difference between the red and NIR reflectances.

Canopy combinations	NIR (.81-.84um)					Red (.65-.67um)					Percent difference				
	Solar zenith angle														
	30^0	38^0	45^0	54^0	60^0	30^0	38^0	45^0	54^0	60^0	30^0	38^0	45^0	54^0	60^0
Shinnery oak-Grass	15.1	11.1	7.7	11.2	13.0	17.9	16.8	16.3	14.9	15.9	18.6	51.3	111.	23.0	22.3
Shinnery oak-Rough coldenia	45.2	44.8	43.0	45.7	42.7	55.2	56.8	57.8	58.6	56.7	22.1	26.7	34.4	28.2	32.7
Shinnery oak-Snakeweed	13.5	10.9	10.0	13.1	14.6	11.3	10.8	11.1	12.2	12.9	20.1	0.9	11.0	-7.3	-13.
Shinnery oak-Creosote	19.5	-	12.7	14.1	12.6	22.6	-	18.9	20.8	24.8	15.8	-	48.8	47.5	96.8
Grass-Rough coldenia	30.1	33.9	35.4	34.7	30.0	32.3	40.1	41.7	45.8	40.8	23.9	24.1	17.5	26.2	36.0
Grass-Snakeweed	2.1	2.4	2.8	2.3	2.0	6.6	5.9	5.3	3.1	3.1	214.	145.	85.7	34.7	55.0
Grass-Creosote	4.9	-	5.7	3.7	3.5	5.2	-	3.6	5.9	9.8	6.1	-	58.3	56.7	78.0
Rough coldenia-Snakeweed	31.7	33.9	33.1	28.3	32.8	43.9	46.0	46.7	46.3	43.8	38.4	35.6	47.1	42.4	54.0
Rough coldenia-Creosote	25.8	-	30.4	31.5	30.2	32.6	-	39.3	37.9	32.3	26.3	-	29.2	20.3	6.9
Snakeweed-Creosote	6.3	-	3.0	1.5	3.3	11.4	-	8.0	8.6	12.2	80.9	-	166.	473.	269.

trend may be explained by examining the bidirectional reflectance distribution of the plant canopies. As previously indicated and discussed in detail in Section 4.1, the backscatter direction of the vegetation canopies shows increasing reflectance with increasing view angles for all canopies. The reflectance in the forward scatter direction is shown to decrease generally with small solar zenith angles and slightly increases with larger solar zenith angles. However, the magnitude of the reflectance increases in the backscatter direction varies substantially while reflectances in the forward scatter direction occur in a narrow range of values as an examination of Appendix 5 indicates. Thus, the Euclidean distances between vegetation canopies are more pronounced in the backscatter direction.

4.3.2 Comparisons in the Forward Scatter Direction

An evaluation of the data presented in Appendix 5 indicates highest Euclidean distances between canopies are generally found in the forward scatter direction of the NIR. The highest single value within the forward scatter varies from one plant canopy to another. These results

were also indicated by the t-test for significant differences between plant canopies. A visual inspection of the NIR bidirectional reflectance distributions indicate two trends:

1) a symmetrical relationship exists in the backscatter direction of the plant canopies, and

2) reflectance values for the plant canopies are similar in magnitude in the backscatter direction.

Although reflectance values are lower in the forward scatter direction, the range of reflectance values are greater resulting in higher Euclidean distances.

4.3.3 Comparisons of Paired Vegetation Canopies

An examination of Appendix 5 indicates that each paired vegetation cover type in the red spectral region shows consistently higher Euclidean distances values than the NIR. Except for the shinnery oak-snakeweed canopy combination, all vegetation cover pairs display this characteristic. This trend is represented in Tables 4.2 and 4.3 which further illustrates the magnitude of these differences when multiple view angle Euclidean distances

are calculated. The Euclidean distances for two multiple combinations of view angles in the backscatter direction for the NIR and red regions and their percent change in values are presented in Tables 4.2 and 4.3. The red spectral region shows a substantial percentage increase in Euclidean distances over the NIR in both cases.

An examination of the NIR bidirectional reflectance of the vegetation canopies in Figs. 4.1-4.5 suggests a reason for the NIR showing less Euclidean distances. Figs. 4.2-4.5 present similar trends in the NIR for all the vegetation canopies except the rough coldenia. In particular, the backscatter direction for these canopies exhibit an exponential increase in reflectance from nadir towards the backscatter direction. Although the absolute values of reflectance increases, the systematic trend remains constant. The distances between reflectance curves between canopies are displaced either relatively higher or lower but at a constant displacement on the reflectance axis. Thus, Euclidean distances are found to be relatively constant from nadir to 45 degrees in the backscatter direction. This can be seen, for example, the shinnery oak-creosote combination shows Euclidean distances relatively constant with off-nadir angles.

The red spectral region shows a somewhat similar reflectance trend as in the NIR, however, the magnitude of reflectance values is dramatically different in each vegetation canopy as seen in Figs. 4.1-4.5. The reason that the red band shows greater variability in reflectance is likely due to the red spectral region being more sensitive to plant canopy parameters. For example, agricultural scenes including soils and agricultural covers shows greatest contrast in the red spectral region (Myers, 1983). The effect of soil is more pronounced in the red than NIR spectral region because soil reflectance peaks in approximately the red spectral region (Myers, 1983). The percent plant cover has a substantially greater effect on the plant canopy reflectance in the red spectral region. This is clearly indicated by the bidirectional reflectance of rough coldenia in the red spectral region compared with plant canopies that have higher plant densities . For example, shinnery oak and snakeweed with approximately 50 percent plant densities have substantially lower reflectances than the rough coldenia canopy. Plant canopies show the greatest contrast in the red spectral range due to chlorophyll absorption which ranges from 70 to 90 percent (Swain and davis, 1978). The high but variable chlorophyll

absorption results in lower reflectances than the NIR, however, it may be argued that the greater variability in absorption results in a wider range of reflectance values for different plant canopies while the NIR reflectances remain constant between 45-50 percent. Thus, the greater sensitivity to vegetation and soil in the red spectral region provides greater Euclidean distances between plant canopies.

4.4 Summary of Results

The major findings of the analyses may be summarized as follows:

1) Bidirectional reflectance patterns can be attributed to the combination of bare soil and complete canopy characteristics. The bidirectional reflectance distribution of bare soil shows a strong linear relationship between reflectance and off-nadir view angles in both the forward and backscatter direction. The bidirectional reflectance distribution of complete vegetation shows an exponential increase in reflectance in the backscatter direction with increasing off-nadir view angles. However, in the forward scatter direction,

bidirectional reflectance shows greater variability than in the backscatter direction. Minimum reflectance occurs at larger off-nadir view angles at small solar zenith angle and approaches nadir as the solar zenith angle increases.

2) The importance of leaf angle distribution in the nature of bidirectional reflectance is indicated by the contrasting BDR patterns associated with grasses (erectophile leaf orientation) and the other vegetation covers (spherical leaf orientations). These differences are most evident at small solar zenith angles. The solar illumination of bare soil at small solar zenith angles in an erectophile canopy is much greater than that found in plant canopies with spherical leaf orientations. It was suggested that canopy architecture accounted for the reflectance distribution of grass in small solar zenith angles being closer to that of a bare soil while plant canopies with spherical leaf orientations resembled the bidirectional reflectance distribution of complete vegetation canopies.

3) Examining separability on an individual band basis, maximum contrasts in reflectances between plant canopies occurs in the red spectral region. Although the NIR of the plant canopies has substantially larger values than

the red spectral region, most of the NIR bidirectional reflectance patterns are similar in shape and magnitude of reflectance values in all the canopies. The red spectral region has a lower reflectance distribution than the NIR pattern, but the reflectance values are much more variable. This can be explained by the high, but variable absorption characteristics of plant canopies in the red spectral region, where as NIR reflectances are found generally between 45-50 percent.

4) The highest contrasts in reflectance in the red spectral region occurs in the backscatter direction, while in the NIR, contrasts in reflectance are highest in the forward scatter direction. The effects of shadowing in the red spectral region masks differential reflectances between canopies in the forward scatter direction, while in the backscatter direction shadowing is at a minimum. However, the extent of shadowing in the forward scatter direction of the NIR is substantially affected by the optical properties of plant canopies.

5 CONCLUSIONS

This research was an attempt to evaluate the bidirectional reflectance patterns of plant canopies and the effect these bidirectional reflectance distributions have on discrimination. In analysis of inter-canopy characteristics, the t-test was used to test significant differences in reflectance between 1) off-nadir view angles and nadir, and 2) bidirectional reflectance variability with changes in solar zenith angle. The second analysis examined intra-canopy reflectance separability using the t-test to determine significant differences in mean reflectances. Euclidean distance quantified the distances between mean canopy reflectance values in multidimensional feature space.

The results of this investigation are in general agreement with findings documented in earlier field based and modeling studies of BDR. For example, increasing reflectance with off-nadir viewing in the NIR and red spectral region has been shown in field studies by Kimes (1983) and Kirchner, et al, (1981). Also, BRF variability with solar zenith angle increases has been reported. Specifically, the shift of minimum reflectance in the

forward scatter direction of plant canopies in both the NIR and red spectral regions closer to nadir with increasing solar zenith angles, as previously reported by Kimes (1983), has been substantiated in this study. Solar zenith angle variability also was shown to increase with sparser vegetation canopies. Within sparse vegetation canopies, the scattering properties of bare soil was found to dominate the BDR of most plant canopies at small solar zenith angles. This had previously been demonstrated by Kimes (1983) in a study of North African vegetation canopies. However, the extent of bare soil influence on the BDR of plant canopies was found to vary with the plant canopies due to their leaf angle distribution. Kimes (1984), using bidirectional reflectance simulation models, suggested that leaf angle orientations having unique BRDF, will be useful in discrimination of plant canopies. It is clear from this field study using the PARABOLA that the grass canopy (erectophile leaf angle distribution) has a distinctly different BDR than the canopies with spherical leaf orientations (eg. shinnery oak) at small solar zenith angles. These differences in BDR due to leaf angle orientation is clearly indicated in the analyses of spectral separability using Euclidean distance. The greatest separability between the grass canopy

(erectophile) with plant canopies with spherical leaf orientations was indicated at small solar zenith angles.

Given the limitations of this study in terms of sample size and limited variability in canopy conditions, these results should be regarded as preliminary findings. The strong indication that enhanced feature discrimination may be achieved under some conditions by using off-nadir observations justifies further research.

While data obtained from the PARABOLA will clearly help in establishing empirical relationships in the BDR characteristics of different canopies, the use of reflectance models such as the SAIL model (Scattering from Arbitrarily Inclined Leaves) of Verhoeff and Bunnik (1981) is likely to be indispensible in pursuing this research. Data obtained from the PARABOLA may be beneficial in testing and validating such models. Where model output does not agree with field observations, modifications may be introduced and if necessary, the fundamental relationship used to define BRF may be re-evaluated.

While this study has helped focus attention on the potential increase in information and discrimination

within and between plant canopies, researchers also need to reassess previous work based on the erroroneous assumption of isotropic surface reflectance. As previously suggested by Kimes (1983) and demonstrated in this research, nadir measurements will not represent accurately hemispherical albedo.

Errors inherent in the basic data, reflectances, are directly transferable to the information which is extracted from these data. In order to minimize the possibility of making incorrect decisions based on such information, it is necessary to eliminate as much uncertainty as possible in the basic measurements. Furthermore, if off-nadir observations are able to enhance feature discrimination, then the future design of satellite systems will have to address this possibility.

6 REFERENCES

Allen, W., Gayle, T., and Richardson, A., 1970. Plant canopy irradiance specified by the Duntley equations. Journal of the Optical Society of America,60: 372-376.

Barnsley, M.J., 1984. Effects of off-nadir view angles on the detected spectral response of vegetation canopies. International J. of remote Sensing, 5: 715-728.

Bird, Richard E., 1984. A simple, solar spectral model for direct-normal and diffuse horizontal irradiance. Solar Energy, 32(4): 461-471.

Brennan, B. and Bandeen, W.R., 1970. Anisotropic reflectance characteristics of natural earth surfaces. Applied Optics, 9:405-412.

Carter, D.B., Schmmudde, T.H. and Sharpe, D.M., 1972. The interface as a working environment-a purpose for physical geography. AAG Technical Paper No. 7.

Colwell, John E., 1974. Vegetation canopy reflectance. Remote sensing of Environment, 13: 475-486.

Coulson, Kinsell L., 1966. Effects of reflection properties of natural surfaces in aerial reconnaissance. Applied Optics, 5(6): 905-917.

Coulson,K.L., Bouricius, G.M., and Gray, E.L., 1965. Optical reflection properties of natural surfaces. Journal of Geophysical Research, 70(18):

Deering, D.W., Lecne, P., 1984. A sphere-scanning radiometer for rapid directional measurements of sky and ground radiance. NASA Technical Memorandum 86171. NASA Goddard Space Flight Center, Greenbelt, MD.

Dittemore, Jr., W.H. and Blum, E.L., 1964. Soil Survey of Ward County, Texas. USDA, Soil Conservation Service.

Egbert, D.D., 1977. A practical method for correcting bidirectional reflectance variations. Proceedings of Machine Processing of Remote Sensing Data, LARS Purdue University,173-186.

Egbert. D.D. and Ulaby, F.T., 1972. Effects of angles on reflectivity. Photogram. Engr. and Remote Sensing, 38:556-564.

Fan, Hansel, 1979. An overview of landuse data availability and accuracy. Remote Sensing Quarterly, 1(3): 7-13.

Jackson, R.D., Pinter, P.J., Idso, S.B., and Reginato, R.J., 1979. Wheat spectral reflectance: interactions between crop configuration, sun elevation and azimuth angle. Applied Optics, 18(22):3730-3732.

Jayroe, Jr., Robert R., 1983. Some observations about Landsat digital analysis. NASA Technical Memorandum No. 78184, George C. Marshall Space Flight Center, Alabama.

Jensen, John R., 1983. Biophysical remote sensing. Annals of the Association of American Geographers, 73(1): 111-132.

Kimes, D.S., 1983. Dynamics of bidirectional reflectance factor distribution for vegetation canopies. Applied Optics, 22(9):1364-1372.

_____, 1984. Modeling the directional reflectance from complete homogeneous vegetation canopies with various leaf-orientation distributions. Journal of the Optical Society of America, 1(7):725-737.

Kimes, D.S., Holben, B.N., Tucker, C.J. and Newcomb, W.W., 1984. Optimal directional view angles for remote sensing missions. International J. of Remote Sensing, 5(6): 887-908.

Kimes, D.S., Smith, J.A., and Ranson, K.J., 1980. Vegetation reflectance measurements as a function of solar zenith angle. Photogram. Engr. and Remote Sensing, 46(12): 1563-1573.

Kirchner, J.A., Schwetzler, C.C., and Smith, J.A., 1981. Simulated directional radiances of vegetation from satellite platforms. International J. of Remote Sensing, 2(3): 253-264.

Kirchner, J.A., Kimes, D.S. and McMurtrey, J.E., 1982. Variation of directional reflectance factors with structual changes of a developing Alfalfa canopy. Applied Optics, 21:3766-3774.

Kirchner, J.A., Youkhana, S. and Smith, J.A., 1982. Influence of sky radiance distribution on the ratio technique for estimating bidirectional reflectance. Photogram. Engr. and Remote Sensing, 48(6): 955-959.

Kriebel, Kark T., 1976. On the variability of the reflected radiation field due to differing distributions of the irradiation. Remote Sensing of the Environment, 4:257-264.

_____, 1978. Measured spectral bidirectional reflection properties of four vegetated surfaces. Applied Optics, 17(2): 253-259.

_____, 1978. Average variability of the radiation reflected by vegetated surfaces due to differing irradiations. Remote Sensing of Environment, 7:81-83.

Latty, R.S. and Hoffer, R.M., 1981. Computer-based

classification accuracy due to data spatial resolution using per-point versus per-field classification techniques. Proceedings of the Machine Processing of Remotely Sensed Data Symposium, 384-393.

Lillessand, T.M. and Kiefer, R.W., 1979. Remote Sensing and Image Interpretation. John Wiley and Sons, Inc., New York.

Mabry, T.J., Hunziker, J.H., and Difeo, Jr., D.R., 1977. Creosote Bush: Biology and Chemistry of Larrea in New World Deserts. Dowden Hutchinson and Ross, Inc. Stroudsburg, Pennsylvania.

Markham, B.L. and Townshend, J.R.G., 1981. Land cover classification accuracy as a function of sensor spatial resolution. Proceedings of the 15th Int. Symposium on Remote Sensing of Environment, Ann Arbor, MI, 1075-1090.

Mendenhall, William, 1971. Introduction To Probability and statistics. Wadsworth Publishing Co., Belmont, CA.

Myers, Victor I., 1983. Remote sensing applications in agriculture. Manual of Remote Sensing II: 2111-2228.

Newman, Allen, 1964. Soil Survey of Cochran County, Texas. USDA, Soil Conservation Service.

Nicodemus, F.E., Richmond, J.C. Hsia, J.J., Ginsberg, I.W. and Limperis, T., 1977. National Bureau of Standards Monogr., No. 160, Washington, DC.

Ott, W., Pfeiffer, B., and Quiel,F., 1984. Directional reflectance propertieOs determined by analysis of airborne multispectral scanner data and atmospheric correction. Remote Sensing of environment, 16: 47-54.

Paludan, Charles, 1975. Geographic research from earth orbit-with special emphasis on land-use. University of Denver, PhD in Geography, University Microfilms Intl., Ann Arbor, MI.

Rao, V.R., Brach, E.J. and Mack, A.R., 1979. Bidirectional reflectance of crops and the soil contributions. Remote Sensing of Environment, 8:115-125.

Ranson, K.J., Vanderbilt, V.C., Biehl, L.L., Robinson, B.F. and Bauer, M.E., 1981. Soybean canopy reflectance as a function of view and illumination geometry. Presented at

the Fifthteen International Symposium on Remote Sensing of Environment, Ann Arbor, MI.

Richardson, A.J., Wiegand, C.L., Gausman, H.W., Cuellar, J.A. and Gerbermann, A.H., 1975. Plant, soil, and shadow reflectance components of row crops. Photogram. Engr. and Remote Sensing, 41 (11): 1401-1407.

Risser, P.G., Birney, E.C., Blocker, H.D., May, S.W., Parton, W.J., and Wiens, J.A.,1981. The True Prairie Ecosystem. Hutchinson Ross Publishing Co., Stroudsburg, PA.

Rosenfield, G.H., 1981. Analysis of variance of thematic mapping experiment data. Photogram. Engr. and Remote Sensing, 47(12): 1685-1692.

Sadowski,F.G., Malila, W.A., Sarno, J.E. and Nalepa, R.F., 1977. The influence of multispectral scanner spatial resolution on forest feature classification. Proceedings of the 11th International Symposium of remote Sensing of Environment, 1279-1288.

Salomonson, Vincent V., 1966. Anisotropy of reflected solar radiation from various surfaces as measured with an

aircraft-mounted radiometer. Proceedings of the 4tn International Symposium of Remote Sensing,393-407.

Salomonson, V.V. and Marlatt, W.E., 1971. Airborne measurements of reflected solar radiation. Remote Sensing of Environment, 2: 1-8.

Schnetzler, C.C., 1981. Effect of sun and sensor geometry, canopy structure and density, and atmospheric condition on the spectral response of vegetation with particular emphasis on across-track pointing. International Society for Photogrammetry and Remote Sensing, International Colloquium, Avignon, France.

Smith, J.A. and Berry, J.K., 1979. Optical diffraction analysis for estimating foliage angle distribution in grassland canopies. Aust. J. of Botany, 27: 123-133.

Smith, J.A. and Oliver, R.E., 1972. Plant canopy models for simulating composite scene spectroradiance in the 0.4 to 1.05 micrometer region. Proceedings of the 8th International Symposioum on Remote Sensing of Environment, Ann Arbor,MI, 1333-1353.

_____,1974. Effects of changing canopy directional reflectance on feature selection. Applied Optics, 13(7): 1599-1604.

Smith, J.A., and Ranson, K.J., 1979. MRS Literature Survey of Bidirectional reflectance, ORI, Inc. Contract Report to NASA/GSFC, Greenbelt, MD.

Staenz, K., Ahern, F.J. and Brown, R.J., 1981. The influence of illumination and viewing geometry on the reflectance factor of agricultural targets. Proceedings of the 15th International Symposium on Remote Sensing of the Environment, Ann Arbor, MI, 867-875.

Stubbendieck, J., Hatch, S.L. and Kjar, K.J., 1981. North American Range Plants, University of Nebraska Press, Lincoln and London.

Suits, G.H., 1972. The calculation of the directional reflectance of a vegetative canopy. Remote Sensing of Environment, 2: 117-125.

Swain, P.H. and Davis, S.M., 1978. Remote Sensing: The Quantitative Approach, McGraw-Hill, New York.

Swain, P.H. and King, R.C., 1973. Two effective feature selection criteria for multispectral remote sensing. Proceedings of First International Joint Conference on Pattern Recognition, IEEE 536-540. Townsend, John R.G., 1984. Agricultural land-cover discrimination using thematic spectral bands. International J. of Remote Sensing, 5(4): 681-698.

Thorne, B. Michael, 1980. Introductory Statistics for Psychology. Duxbury Press, North Scituate, MA.

Tucker, C.J., 1978. A comparison of satellite sensor bands for vegetation monitoring. Photogram. Engr. and Remote Sensing, 44(11): 1369-1380.

Verhoeff, W, Bunnik, N.J.J., 1981. Influene of crop geometry on multispectral reflectance determined by use of canopy reflectance models. Proceedings, International Colloquium on Signatures of Remotely Sensed Objects, Avignon, France, pp 273-290.

Williams, Darrel L., Irons, J.R., Markham, B.L., Nelson, R.F., Toll, D.L., Latty, R.S. and Stauffer, M.L., 1984. A statistical evaluation of the advantages of landsat TM data in comparison to multispectral scanner data. IEEE Transactions on Geoscience and Remote Sensing, GE-22(3):294-302.

Wright, H.A.and Bailey, A.W., 1982. Fire Ecology.,John Wiley and Sons, New York.

7 APPENDICES

Appendix 1 : Calculated transformed divergence values for selected canopy combinations using the red and NIR spectral regions for solar zenith angles of a) 30 degrees and b) 38 degrees

		View angle						
	Canopy combination	-45^0	-30^0	-15^0	0^0	$+15^0$	$+30^0$	$+45^0$
a)	Shinnery oak-Grass	2000	2000	2000	2000	2000	2000	2000
	Shinnery oak-Rough coldenia	2000	2000	2000	2000	2000	2000	2000
	Shinnery oak-Snakeweed	2000	2000	2000	2000	2000	2000	2000
	Shinnery oak-Creosote	2000	2000	2000	2000	2000	2000	2000
	Grass-Rough coldenia	2000	2000	2000	2000	2000	2000	2000
	Grass-Snakeweed	1884	1775	1968	1982	1963	2000	2000
	Grass-Creosote	1886	898	1075	991	2000	1891	1729
	Rough coldenia-Snakeweed	2000	2000	2000	2000	2000	2000	2000
	Rough coldenia-Creosote	2000	2000	2000	2000	2000	2000	2000
	Snakeweed-Creosote	1999	1932	1999	1986	2000	1992	2000
b)	Shinnery oak-Grass	2000	2000	2000	2000	2000	2000	2000
	Shinnery oak-Rough Coldenia	2000	2000	2000	2000	2000	2000	2000
	Shinnery oak-Snakeweed	2000	2000	2000	2000	2000	2000	2000
	Shinnery oak-Creosote	2000	2000	2000	2000	2000	2000	2000
	Grass-Rough coldenia	1098	2000	2000	2000	2000	2000	2000
	Grass-Snakeweed	2000	2000	1580	1971	2000	1990	1991
	Grass-Creosote	2000	2000	754	1550	2000	1714	1991
	Rough coldenia-Snakeweed	2000	2000	2000	2000	2000	2000	2000
	Rough coldenia-Creosote	2000	2000	2000	2000	2000	2000	2000
	Snakeweed-Creosote	2000	2000	1621	1961	2000	1996	2000

Appendix 2 : Percent of shadowing in the principle plane for each vegetation canopy type and view angle for different solar zenith angles

Plant Canopy	Solar zenith angle	View angle											
		-60^0	-50^0	-40^0	-30^0	-20^0	-10^0	$+10^0$	$+20^0$	$+30^0$	$+40^0$	$+50^0$	$+60^0$
Shinnery oak	30^0	10.1	5.4	10.2	21.1	31.2	32.7	30.5	21.2	40.3	40.9	33.2	27.2
	38^0	8.3	15.7	23.2	43.1	33.3	36.0	39.6	48.3	38.0	42.5	39.3	41.2
	45^0	17.3	24.0	27.7	34.8	34.5	41.6	51.0	54.7	49.9	50.9	41.2	39.6
	54^0	9.6	16.2	25.6	27.5	38.6	27.7	59.2	36.5	46.1	53.1	45.4	35.7
	60^0	18.4	29.6	36.9	37.4	50.5	52.7	70.3	49.6	50.6	53.7	43.9	43.7
Grass	30^0	.4	.8	2.4	4.5	3.8	2.2	4.5	13.9	18.0	20.9	22.5	20.6
	38^0	1.9	4.3	6.1	7.6	15.4	17.6	12.8	10.7	20.5	15.1	15.3	13.4
	45^0	4.2	8.3	9.6	12.2	10.8	15.5	19.9	28.8	30.6	29.5	31.1	24.9
	54^0	5.7	6.8	12.3	15.8	22.0	44.0	20.8	16.6	24.5	20.7	25.5	22.8
	60^0	11.8	19.2	28.3	24.9	31.5	17.7	36.6	32.5	28.0	30.5	37.3	28.9
Snakeweed	30^0	0.0	1.1	8.8	14.3	18.0	4.4	31.6	28.8	24.6	22.6	27.3	22.4
	38^0	.9	2.7	6.1	12.6	14.1	26.6	23.3	32.5	27.1	28.1	28.8	26.8
	45^0	1.7	6.3	17.4	20.7	19.0	26.9	39.9	25.9	36.8	30.3	27.4	27.0
	54^0	4.5	7.6	15.2	23.0	17.4	42.1	26.6	35.5	34.5	33.9	31.1	27.2
	60^0	15.0	24.6	30.2	29.2	28.2	52.7	49.9	35.1	49.1	35.5	34.2	28.6
Rough coldenia	30^0	1.0	0.6	0.6	0.0	3.2	0.0	2.0	1.8	7.7	8.1	10.4	7.8
	38^0	0.0	0.2	0.0	0.3	1.2	0.0	6.6	5.9	5.5	6.0	5.7	9.6
	45^0	0.8	3.1	2.7	4.5	4.5	2.2	6.6	7.4	6.2	18.8	8.1	13.1
	54^0	0.3	0.2	4.9	8.4	8.3	2.2	3.3	6.6	18.7	12.0	12.5	12.6
	60^0	5.7	13.8	14.0	7.6	10.2	26.6	16.6	5.5	14.0	16.1	15.5	19.6
Creosote	30^0	4.9	1.7	0.6	1.4	5.6	11.1	4.1	5.5	23.7	28.2	10.9	23.6
	45^0	14.8	19.0	25.6	28.8	32.8	60.3	46.6	33.3	32.1	43.8	28.9	41.1
	54^0	12.7	15.7	14.7	20.1	20.1	8.3	37.4	25.9	26.5	36.1	31.9	39.6
	60^0	16.3	20.6	18.9	20.7	20.7	37.7	32.1	25.1	38.0	34.4	30.1	47.8

Appendix 3 : Students t-values for the comparison between off-nadir and nadir mean reflectances (red and NIR) for selected solar zenith angles for a) rough coldenia, b) creosote c) grass, d) shinnery oak and e) snakeweed. (Underlined values indicate significance at the 99 percent level.)

a)

CHANNEL 1

Solar zenith angle	View angle						
	-45^0	-30^0	-15^0	0^0	$+15^0$	$+30^0$	$+45^0$
30^0	8.7	6.8	2.8	-	5.5	10.2	11.2
38^0	11.7	6.6	3.1	-	5.3	10.3	10.6
45^0	12.2	5.8	3.4	-	1.6	5.4	11.0
54^0	12.8	9.4	2.7	-	2.1	3.7	6.4
60^0	17.5	9.0	3.7	-	3.2	5.3	8.0

CHANNEL 2

Solar zenith angle	View angle						
	-45^0	-30^0	-15^0	0^0	$+15^0$	$+30^0$	$+45^0$
30^0	11.7	6.6	3.1	-	5.3	10.3	10.6
38^0	9.9	5.8	3.0	-	0.1	5.0	7.8
45^0	14.4	10.2	3.4	-	1.9	4.1	6.7
54^0	19.6	10.3	3.6	-	3.2	4.5	5.9
60^0	13.1	5.5	2.4	-	2.6	4.4	6.3

b)

CHANNEL 1

Solar zenith angle	View angle						
	-45^0	-30^0	-15^0	0^0	$+15^0$	$+30^0$	$+45^0$
30^0	2.8	2.7	0.5	-	1.0	0.4	0.5
45^0	4.2	1.6	0.7	-	0.2	0.1	0.7
54^0	5.1	3.0	0.9	-	0.4	0.6	0.0
60^0	2.4	1.8	0.6	-	1.2	2.1	2.7

CHANNEL 2

Solar zenith angle	View angle						
	-45^0	-30^0	-15^0	0^0	$+15^0$	$+30^0$	$+45^0$
30^0	4.9	3.2	0.9	-	1.6	2.5	2.4
45^0	8.2	4.0	1.3	-	0.6	0.6	1.2
54^0	13.1	5.3	1.2	-	0.4	0.3	1.5
60^0	11.6	4.8	2.9	-	0.1	1.2	0.5

c)

CHANNEL 1

Solar zenith angle	View angle						
	-45^0	-30^0	-15^0	0^0	$+15^0$	$+30^0$	$+45^0$
30^0	3.6	4.1	2.5	-	1.4	2.9	6.0
38^0	5.3	3.9	1.5	-	1.9	3.1	3.7
45^0	7.2	5.4	2.4	-	1.1	1.6	3.4
54^0	10.3	7.4	2.2	-	1.5	2.8	2.1
60^0	14.7	10.1	1.7	-	2.2	2.9	0.5

CHANNEL 2

Solar zenith angle	View angle						
	-45^0	-30^0	-15^0	0^0	$+15^0$	$+30^0$	$+45^0$
30^0	5.0	4.9	2.3	-	1.0	2.6	4.1
38^0	7.3	7.8	2.5	-	1.5	2.6	2.1
45^0	8.3	5.7	.2.5	-	0.1	0.3	0.3
54^0	9.8	4.4	1.5	-	1.2	0.4	0.7
60^0	10.4	3.9	0.5	-	1.7	1.0	1.1

d)

CHANNEL 1

Solar zenith angle	View angle						
	-45^0	-30^0	-15^0	0^0	$+15^0$	$+30^0$	$+45^0$
30^0	14.6	10.9	4.4	-	3.6	8.5	11.8
38^0	14.3	7.9	2.8	-	3.0	8.9	14.3
45^0	7.5	11.2	3.9	-	3.7	7.0	11.1
54^0	9.4	6.7	4.6	-	3.1	7.2	3.1
60^0	18.7	10.7	3.1	-	1.9	3.6	1.0

CHANNEL 2

Solar zenith angle	View angle						
	-45^0	-30^0	-15^0	0^0	$+15^0$	$+30^0$	$+45^0$
30^0	16.7	13.0	4.6	-	2.2	3.0	2.4
38^0	17.7	50.1	10.1	-	3.6	11.5	33.5
45^0	8.3	6.2	1.4	-	1.3	2.4	2.9
54^0	8.7	7.6	2.6	-	3.0	4.2	2.7
60^0	12.4	7.1	1.5	-	1.3	2.7	1.1

e)

CHANNEL 1

Solar zenith angle	View angle						
	-45^0	-30^0	-15^0	0^0	$+15^0$	$+30^0$	$+45^0$
30^0	6.8	5.7	3.1	-	3.2	5.8	7.4
38^0	17.4	10.7	4.0	-	2.1	5.5	7.9
45^0	13.1	7.4	2.8	-	1.9	2.8	2.5
54^0	12.1	6.3	3.0	-	2.9	5.4	6.4
60^0	10.2	5.9	2.8	-	1.5	2.2	1.3

CHANNEL 2

Solar zenith angle	View angle						
	-45^0	-30^0	-15^0	0^0	$+15^0$	$+30^0$	$+45^0$
30^0	19.0	15.7	6.7	-	2.9	2.4	1.1
38^0	29.9	24.0	8.1	-	2.6	2.3	1.2
45^0	35.3	19.9	6.3	-	3.1	1.6	2.9
54^0	38.5	17.3	6.8	-	2.1	2.2	5.2
60^0	62.8	18.8	8.7	-	1.7	1.5	53.4

Appendix 4 : Students t-values for the comparison between pairs of solar zenith angle mean reflectances (red and NIR) for selected view angles for a) rough coldenia, b) creosote, c) grass, d) shinnery oak and e) snakeweed. (Underlined values indicate significance at the 99 percent level.)

a)

	Comparative pairs of solar zenith angles	View angle -45^0	-30^0	-15^0	0^0	$+15^0$	$+30^0$	$+45^0$
CHANNEL 1	$30^0 - 38^0$	2.8	1.7	.18	.46	.79	.29	2.5
	$30^0 - 45^0$	5.1	.77	.46	.76	.03	.55	1.6
	$30^0 - 54^0$	5.5	1.2	1.0	.34	.38	.66	1.6
	$30^0 - 60^0$	5.5	22.	2.2	3.3	3.2	3.5	3.3
	$38^0 - 45^0$	2.2	.54	.32	.39	.72	.27	.15
	$38^0 - 54^0$	2.8	0.0	1.0	.20	.44	.37	.30
	$38^0 - 60^0$	2.6	1.6	2.3	2.5	2.9	2.3	1.4
	$45^0 - 54^0$	.91	.86	.58	.57	.32	.10	.37
	$45^0 - 60^0$	.40	2.8	1.9	1.6	3.0	1.6	1.2
	$54^0 - 60^0$	.57	1.9	1.8	3.1	3.0	1.4	.56
CHANNEL 2	$30^0 - 38^0$	3.6	1.3	.05	.07	2.5	1.1	3.0
	$30^0 - 45^0$	6.9	2.6	.40	.82	.24	1.0	2.2
	$30^0 - 54^0$	8.8	2.0	.71	.13	1.0	.66	1.1
	$30^0 - 60^0$	7.9	.06	1.4	1.2	2.3	3.0	4.3
	$38^0 - 45^0$	2.6	8.5	.55	.55	2.2	.29	.41
	$38^0 - 54^0$	4.5	8.7	.96	.01	1.9	.09	1.0
	$38^0 - 60^0$	4.0	28.	1.7	.95	3.7	1.8	2.5
	$45^0 - 54^0$	2.3	.49	.35	.68	.84	.13	.25
	$45^0 - 60^0$	1.9	2.4	1.2	.48	1.5	1.1	1.3
	$54^0 - 60^0$	.13	1.8	1.0	3.1	2.8	1.1	1.2

b)

	Comparative pairs of solar zenith angles	View angle						
		-45^0	-30^0	-15^0	0^0	$+15^0$	$+30^0$	$+45^0$
CHANNEL 1	$30^0 - 45^0$	.42	1.8	2.9	1.1	.24	.03	1.8
	$30^0 - 54^0$	.79	1.4	1.4	1.8	1.7	.27	1.7
	$30^0 - 60^0$	.13	.02	.28	.09	.44	.83	2.4
	$45^0 - 54^0$	.44	.49	1.2	.52	1.2	.29	.22
	$45^0 - 60^0$	.52	1.3	3.0	1.2	.15	.94	.51
	$54^0 - 60^0$	.86	.97	1.5	1.9	1.3	.73	.75
CHANNEL 2	$30^0 - 45^0$	2.6	.67	1.4	1.4	.36	.10	1.4
	$30^0 - 54^0$	2.7	1.4	1.6	1.8	.35	-	2.2
	$30^0 - 60^0$	2.9	1.5	1.6	2.3	.67	1.9	1.6
	$45^0 - 54^0$	1.0	.45	.34	.25	.02	.07	.32
	$45^0 - 60^0$	.03	.75	.06	.81	.33	1.2	.12
	$54^0 - 60^0$	1.2	.40	.42	.66	.38	1.2	.18

c)

	Comparative pairs of solar zenith angles	View angle						
		-45^0	-30^0	-15^0	0^0	$+15^0$	$+30^0$	$+45^0$
CHANNEL 1	$30^0 - 38^0$	1.0	0.0	1.4	1.1	2.9	2.7	1.9
	$30^0 - 45^0$	1.9	.54	3.7	2.6	2.9	1.3	.81
	$30^0 - 54^0$	2.0	9.4	4.1	3.7	4.1	2.7	2.4
	$30^0 - 60^0$	2.0	7.4	4.6	3.5	4.3	2.6	4.5
	$38^0 - 45^0$	1.1	.44	1.3	1.0	.13	1.6	.43
	$38^0 - 54^0$	1.1	2.7	1.8	1.6	.80	.41	5.3
	$38^0 - 60^0$	.81	2.5	2.1	1.5	1.3	.20	6.7
	$45^0 - 54^0$	.21	2.3	1.0	.77	1.0	1.8	2.5
	$45^0 - 60^0$	.70	2.1	1.6	.61	1.5	1.5	4.3
	$54^0 - 60^0$	.58	.79	.40	.21	.78	.58	2.8
CHANNEL 2	$30^0 - 38^0$	.63	.34	.76	1.5	2.1	1.3	1.4
	$30^0 - 45^0$	2.0	.49	1.9	2.1	1.2	.18	3.0
	$30^0 - 54^0$	3.3	.29	2.1	1.3	1.5	.61	6.1
	$30^0 - 60^0$	4.8	.17	1.5	.23	1.0	1.3	6.9
	$38^0 - 45^0$	1.3	.75	.88	.77	.34	1.1	2.5
	$38^0 - 54^0$	2.5	.51	1.0	.22	.16	1.5	6.6
	$38^0 - 60^0$	3.8	.05	.74	1.3	.45	2.7	6.9
	$45^0 - 54^0$	1.0	.08	.23	.94	.17	.76	3.1
	$45^0 - 60^0$	2.1	.50	.01	1.8	.09	1.6	4.8
	$54^0 - 60^0$	1.0	.36	.16	1.0	.26	.48	3.6

d)

	Comparative pairs of solar zenith angles	View angle						
		-45^0	-30^0	-15^0	0^0	$+15^0$	$+30^0$	$+45^0$
CHANNEL 1	$30^0 - 38^0$	2.8	.85	.70	.68	.22	1.0	1.9
	$30^0 - 45^0$	1.7	2.8	.26	.86	1.5	.68	1.5
	$30^0 - 54^0$	2.2	2.7	4.5	3.1	2.1	4.1	2.1
	$30^0 - 60^0$	1.3	7.1	9.0	4.2	3.1	3.9	8.4
	$38^0 - 45^0$	.39	1.1	.41	.25	1.7	.11	.12
	$38^0 - 54^0$	.72	1.6	1.9	2.9	2.5	1.0	1.7
	$38^0 - 60^0$	1.9	3.8	3.9	4.1	3.8	1.6	7.7
	$45^0 - 54^0$	.23	.98	2.8	2.5	.05	1.0	1.6
	$45^0 - 60^0$	1.3	4.9	5.4	3.7	.44	1.4	6.3
	$54^0 - 60^0$	1.8	1.4	4.7	1.6	.54	.97	1.0
CHANNEL 2	$30^0 - 38^0$	5.7	2.2	2.4	1.0	.50	3.2	3.0
	$30^0 - 45^0$	5.5	1.1	.94	.89	.63	.26	1.6
	$30^0 - 54^0$	4.6	.22	.82	.90	.47	1.2	.65
	$30^0 - 60^0$	12.	2.5	.72	1.1	.08	.32	3.0
	$38^0 - 45^0$	1.6	.89	.42	.49	.83	2.8	6.0
	$38^0 - 54^0$	1.3	.60	.20	.22	.14	.34	3.8
	$38^0 - 60^0$	2.4	1.5	.36	.76	.27	1.4	7.2
	$45^0 - 54^0$	.07	1.0	.48	.35	.81	.98	2.4
	$45^0 - 60^0$	.06	.55	.55	.08	.21	.18	5.8
	$54^0 - 60^0$	.15	1.3	.11	.53	.22	.44	2.2

e)

	Comparative pairs of solar zenith angles	View angle						
		-45^0	-30^0	-15^0	0^0	$+15^0$	$+30^0$	$+45^0$
CHANNEL 1	30^0 - 38^0	3.0	.92	1.5	2.3	.24	.38	1.0
	30^0 - 45^0	5.0	1.6	1.1	1.8	1.3	.73	.27
	30^0 - 54^0	4.1	1.2	2.4	.99	.04	.48	3.5
	30^0 - 60^0	3.7	1.8	2.6	1.7	.52	1.5	7.2
	38^0 - 45^0	2.2	.99	.17	.10	1.3	1.0	.43
	38^0 - 54^0	1.9	.38	.42	1.7	.20	.21	3.4
	38^0 - 60^0	1.7	1.2	.74	-	.34	1.4	9.1
	45^0 - 54^0	.52	.35	.54	1.1	1.3	1.0	2.2
	45^0 - 60^0	.48	.58	.81	.08	1.0	1.7	4.6
	54^0 - 60^0	.02	.73	.50	1.1	.48	.93	4.4
CHANNEL 2	30^0 - 38^0	5.6	1.0	2.3	1.4	.48	.33	.86
	30^0 - 45^0	13.	.65	1.4	.64	.43	.81	3.6
	30^0 - 54^0	17.	.99	.47	.30	.40	1.4	7.5
	30^0 - 60^0	20.	2.8	.14	1.7	3.5	5.6	15.
	38^0 - 45^0	5.9	.51	.78	.77	.12	1.3	3.4
	38^0 - 54^0	8.1	2.0	1.9	2.0	.74	2.0	9.1
	38^0 - 60^0	11.	3.6	2.3	7.0	3.6	6.7	22.
	45^0 - 54^0	3.8	1.7	1.0	1.0	.71	.87	3.3
	45^0 - 60^0	8.6	3.5	1.4	3.0	4.2	6.5	11.
	54^0 - 60^0	5.6	1.9	.59	1.1	2.1	3.4	2.4

Appendix 5 : Matrices of students t-values for comparison of mean reflectances at nadir for different canopies in the red and NIR spectral bands for solar zenith angles a) 30 degrees, b) 38 degrees, c) 45 degrees, d) 45 degrees and e) 60 degrees. (Underlined t-values indicate no differences in reflectance at the 99 percent level).

Red Spectral Region

		Shinnery oak	Grass	Rough coldenia	Snakeweed	Creosote
a)	Shinnery oak	-				
	Grass	7.9	-			
	Rough coldenia	48.8	20.6	-		
	Snakeweed	9.1	3.5	36.9	-	
	Creosote	6.3	1.8	11.1	4.3	-

		Shinnery oak	Grass	Rough Coldenia	Snakeweed
b)	Shinnery oak	-			
	Grass	5.3	-		
	Rough coldenia	34.2	16.8	-	
	Snakeweed	12.9	2.7	13.6	-

		Shinnery oak	Grass	Rough coldenia	Snakeweed	Creosote
c)	Shinnery oak	-				
	Grass	6.9	-			
	Rough coldenia	22.2	18.6	-		
	Snakeweed	5.9	1.9	21.3	-	
	Creosote	4.2	1.8	9.2	2.8	-

		Shinnery oak	Grass	Rough coldenia	Snakeweed	Creosote
d)	Shinnery oak	-				
	Grass	10.1	-			
	Rough coldenia	53.2	37.5	-		
	Snakeweed	13.3	.6	45.1	-	
	Creosote	4.5	1.8	12.8	2.1	-

		Shinnery oak	Grass	Rough coldenia	Snakeweed	Creosote
e)	Shinnery oak	-				
	Grass	11.0	-			
	Rough coldenia	30.8	25.6	-		
	Snakeweed	7.9	1.7	25.7	-	
	Creosote	7.4	4.6	9.0	5.3	-

NIR Spectral Region

		Shinnery oak	Grass	Rough coldenia	Snakeweed	Creosote
a)	Shinnery oak	-				
	Grass	4.4	-			
	Rough coldenia	32.0	11.9	-		
	Snakeweed	9.5	.7	27.0	-	
	Creosote	5.8	2.0	7.9	3.2	-

		Shinnery oak	Grass	Rough coldenia	Snakeweed
b)	Shinnery oak	-			
	Grass	3.3	-		
	Rough coldenia	16.3	12.7	-	
	Snakeweed	19.5	1.1	16.4	-

		Shinnery oak	Grass	Rough coldenia	Snakeweed	Creosote
c)	Shinnery oak	-				
	Grass	1.2	-			
	Rough coldenia	13.9	11.7	-		
	Snakeweed	4.8	1.8	16.5	-	
	Creosote	3.5	2.5	8.3	1.6	-

		Shinnery oak	Grass	Rough coldenia	Snakeweed	Creosote
d)	Shinnery oak	-				
	Grass	3.0	-			
	Rough coldenia	24.8	14.5	-		
	Snakeweed	9.2	1.1	23.8	-	
	Creosote	5.0	1.8	12.6	1.3	-

		Shinnery oak	Grass	Rough coldenia	Snakeweed	Creosote
e)	Shinnery oak	-				
	Grass	3.2	-			
	Rough coldenia	11.8	8.6	-		
	Snakeweed	8.1	0.1	12.4	-	
	Creosote	3.7	0.2	9.3	0.1	-

Appendix 6 : Euclidean distances between canopy pairs for selected view angles and solar zenith angles in the a) red, b) NIR and c) the red and NIR spectral bands.

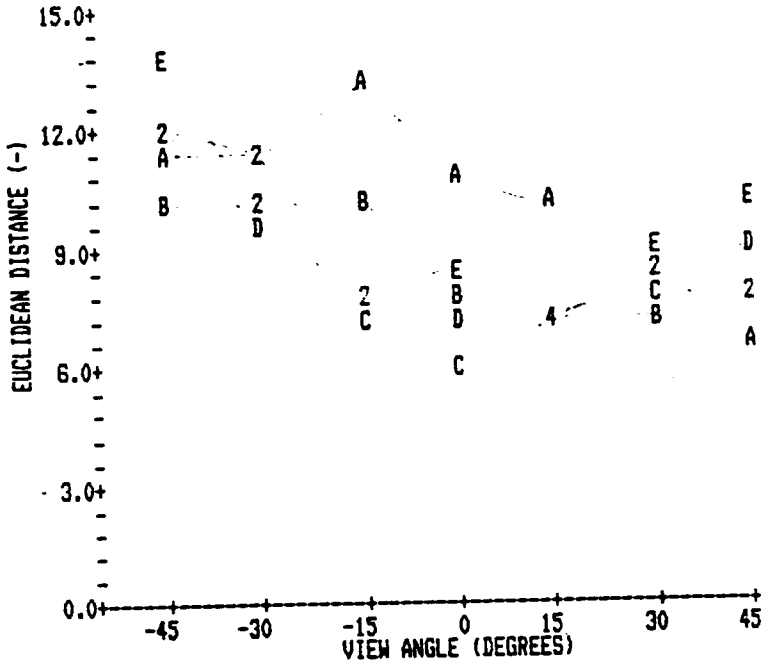
15.0+
12.0+
9.0+
6.0+
3.0+
0.0+
EUCLIDEAN DISTANCE (-)
-45
-30
-15
0
15
30
45
VIEW ANGLE (DEGREES)

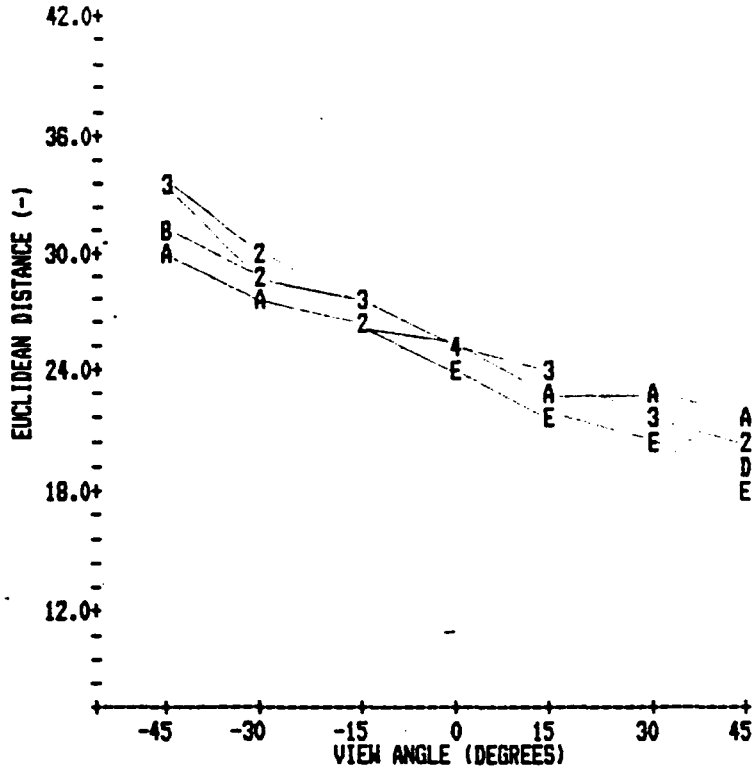
42.0+
36.0+
30.0+
24.0+
18.0+
12.0+
EUCLIDEAN DISTANCE (-)
-45
-30
-15
0
15
30
45
VIEW ANGLE (DEGREES)

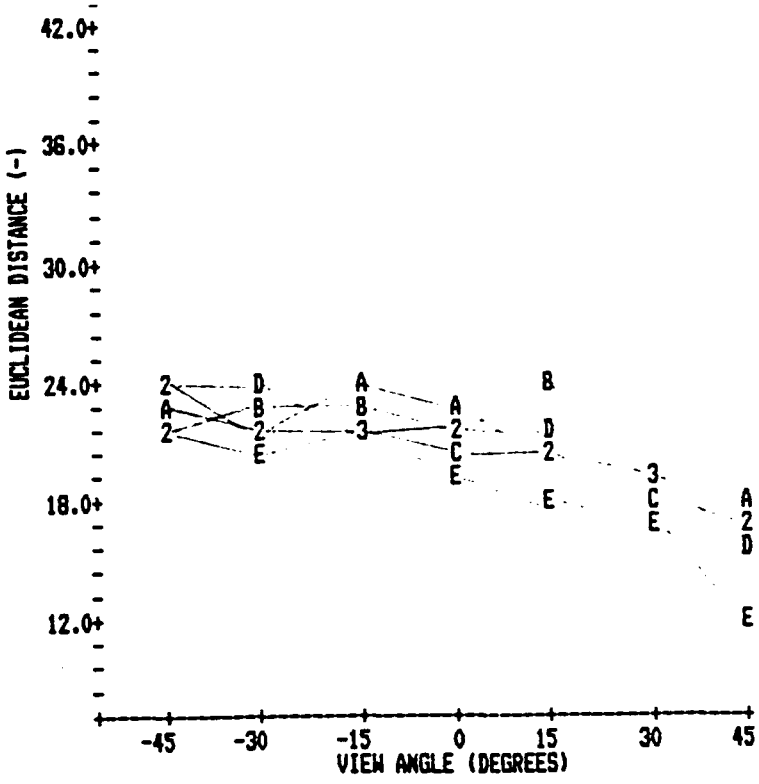
42.0+
36.0+
30.0+
24.0+
18.0+
12.0+
EUCLIDEAN DISTANCE (-)
-45
-30
-15
0
15
30
45
VIEW ANGLE (DEGREES)

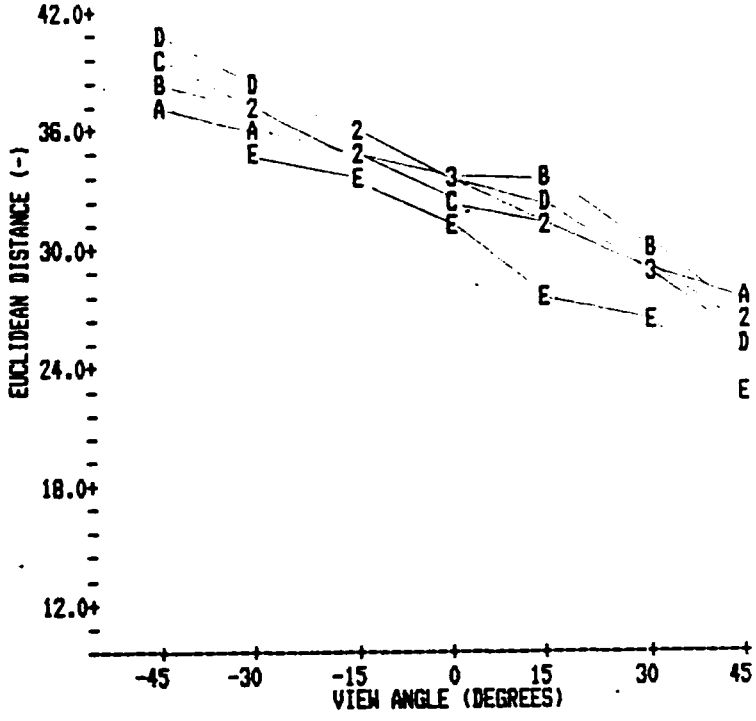
42.0+
36.0+
30.0+
24.0+
18.0+
12.0+
EUCLIDEAN DISTANCE (-)
-45
-30
-15
0
15
30
45
VIEW ANGLE (DEGREES)

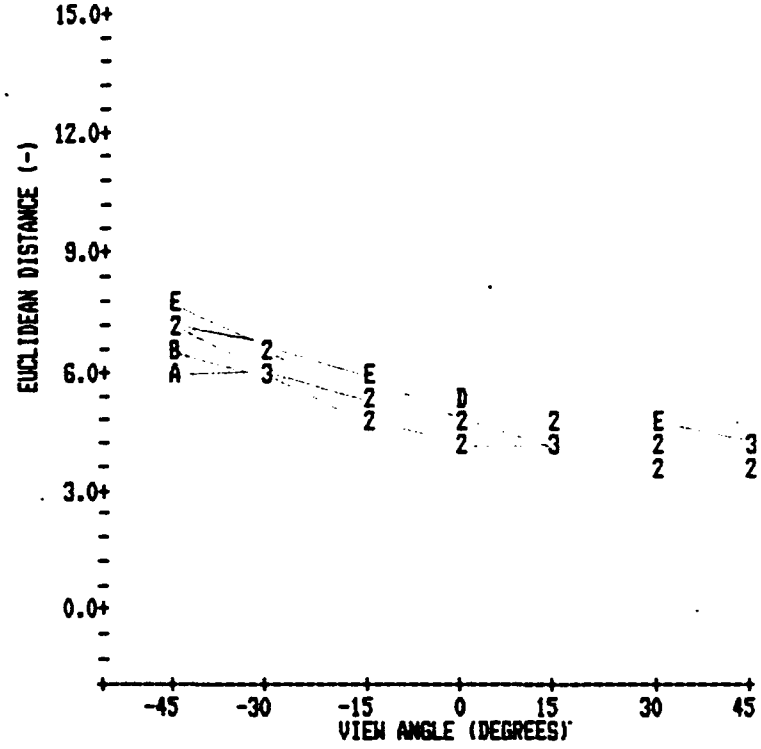
15.0+
12.0+
9.0+
6.0+
3.0+
0.0+
EUCLIDEAN DISTANCE (-)
-45
-30
-15
0
15
30
45
VIEW ANGLE (DEGREES)

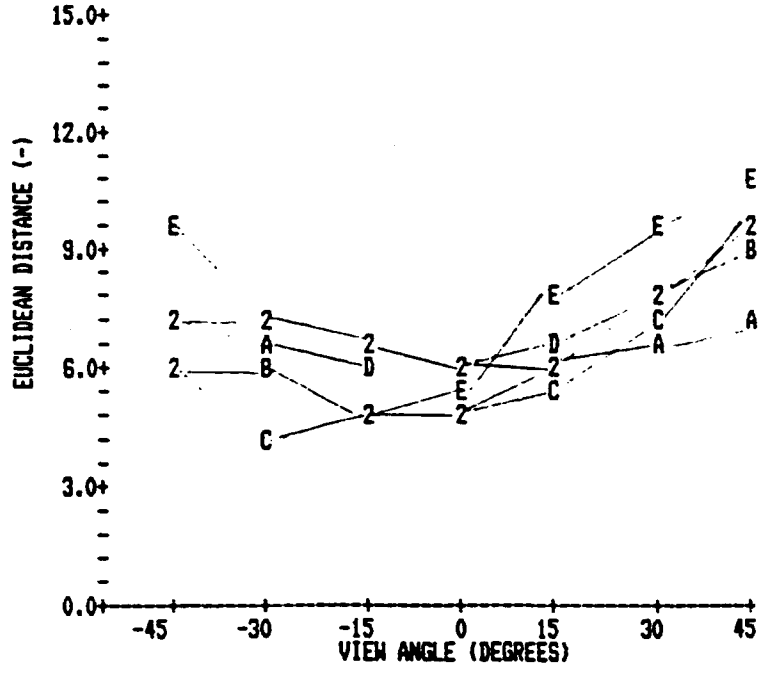
15.0+
12.0+
9.0+
6.0+
3.0+
0.0+
EUCLIDEAN DISTANCE (-)
-45
-30
-15
0
15
30
45
VIEW ANGLE (DEGREES)

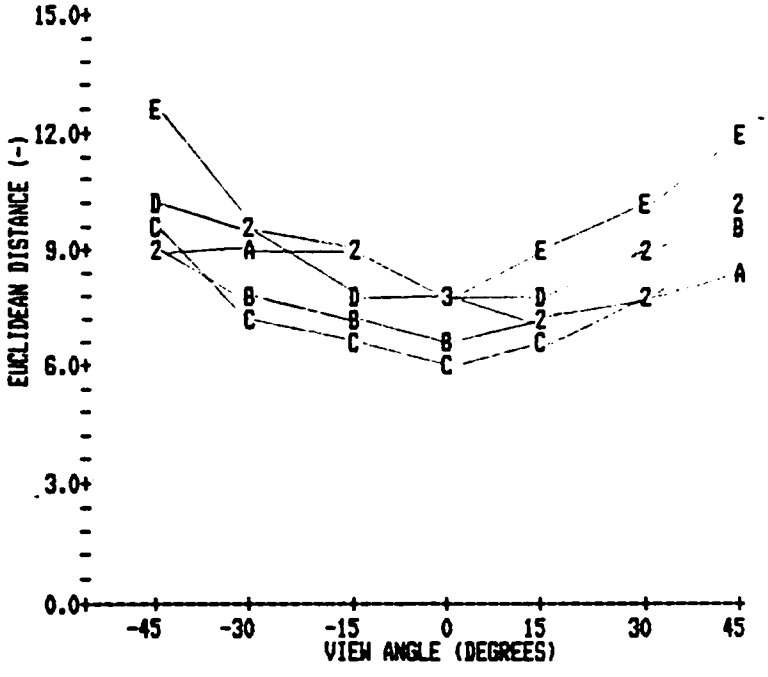
15.0+
12.0+
9.0+
6.0+
3.0+
0.0+
EUCLIDEAN DISTANCE (-)
-45
-30
-15
0
15
30
45
VIEW ANGLE (DEGREES)

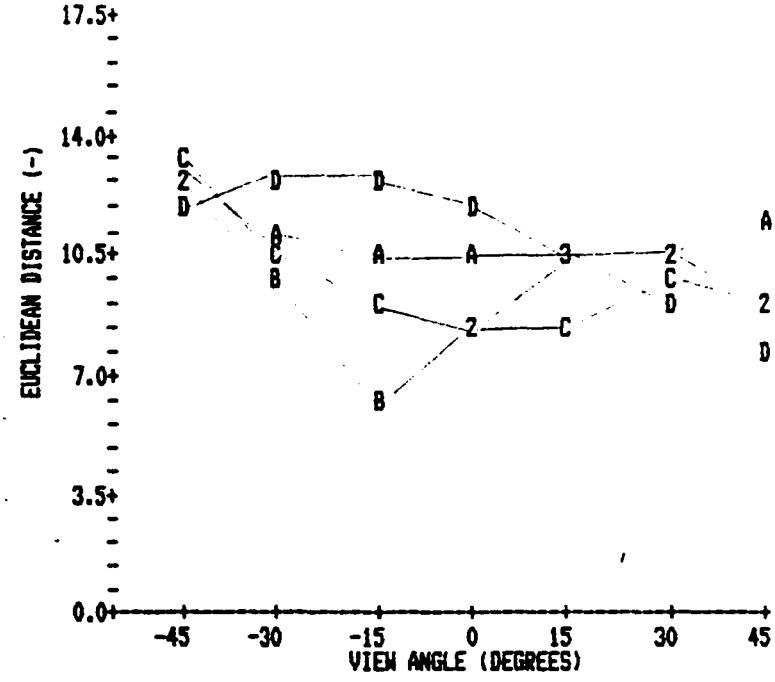
17.5+
14.0+
10.5+
7.0+
3.5+
0.0+
EUCLIDEAN DISTANCE (-)
-45
-30
-15
0
15
30
45
VIEW ANGLE (DEGREES)

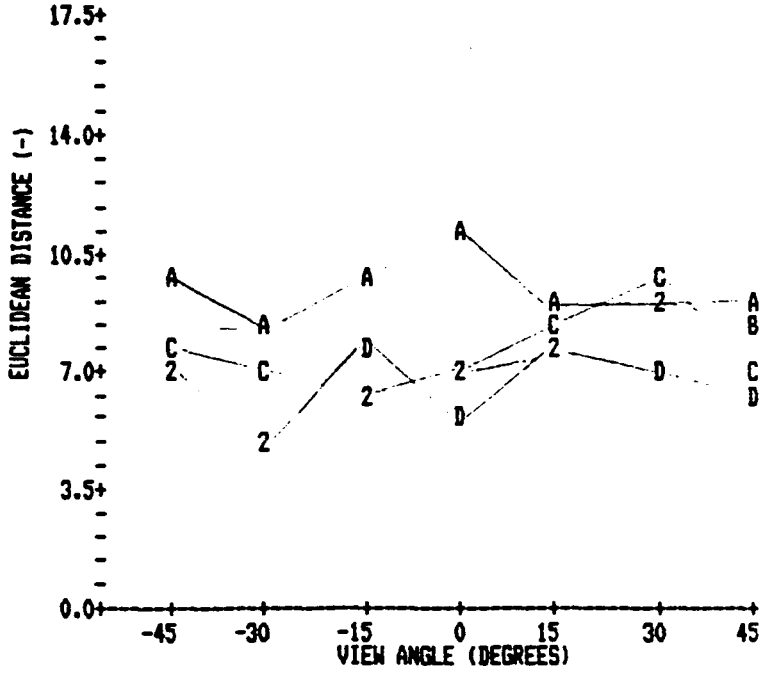
17.5+
14.0+
10.5+
7.0+
3.5+
0.0+
EUCLIDEAN DISTANCE (-)
-45
-30
-15
0
15
30
45
VIEW ANGLE (DEGREES)

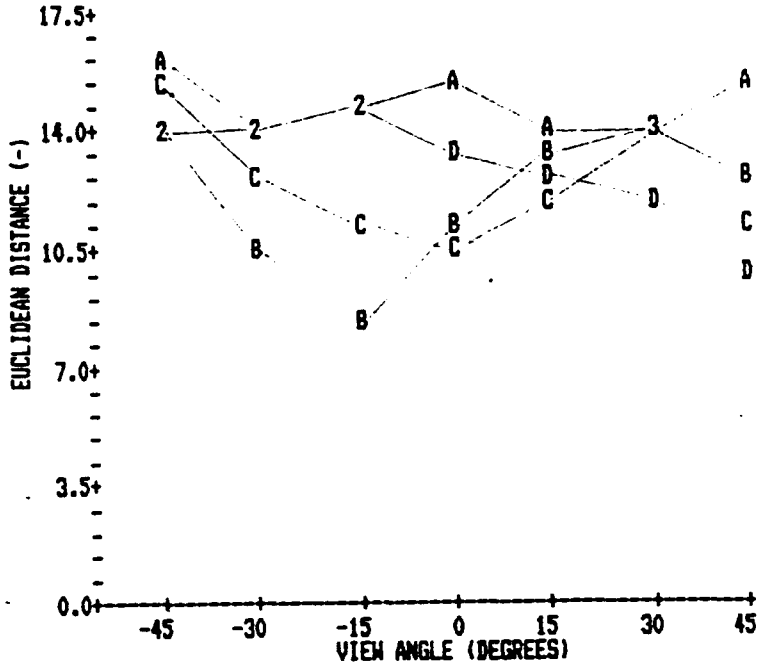
17.5+
14.0+
10.5+
7.0+
3.5+
0.0+
EUCLIDEAN DISTANCE (-)
-45
-30
-15
0
15
30
45
VIEW ANGLE (DEGREES)

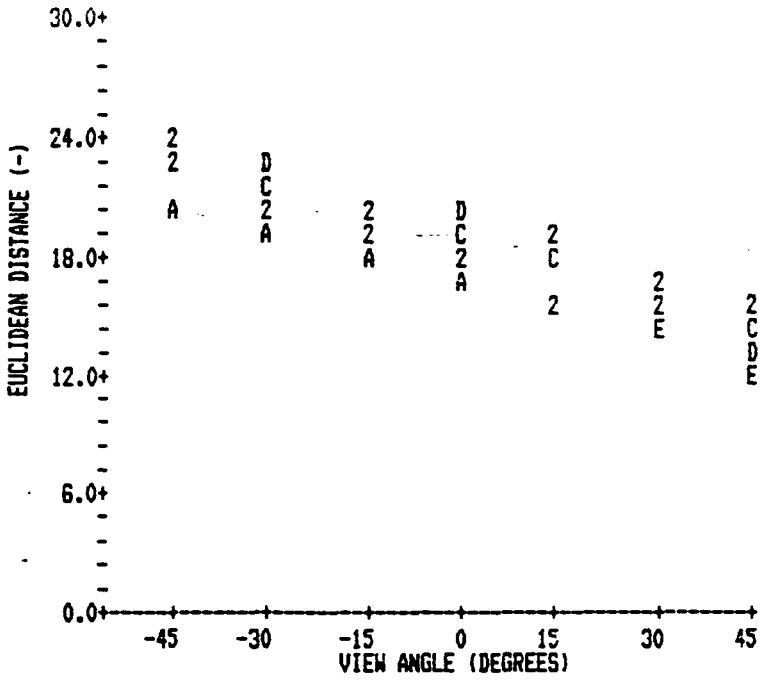
EUCLIDEAN DISTANCE (-)
30.0+
24.0+
18.0+
12.0+
6.0+
0.0+
-45
-30
-15
0
15
30
45
VIEW ANGLE (DEGREES)

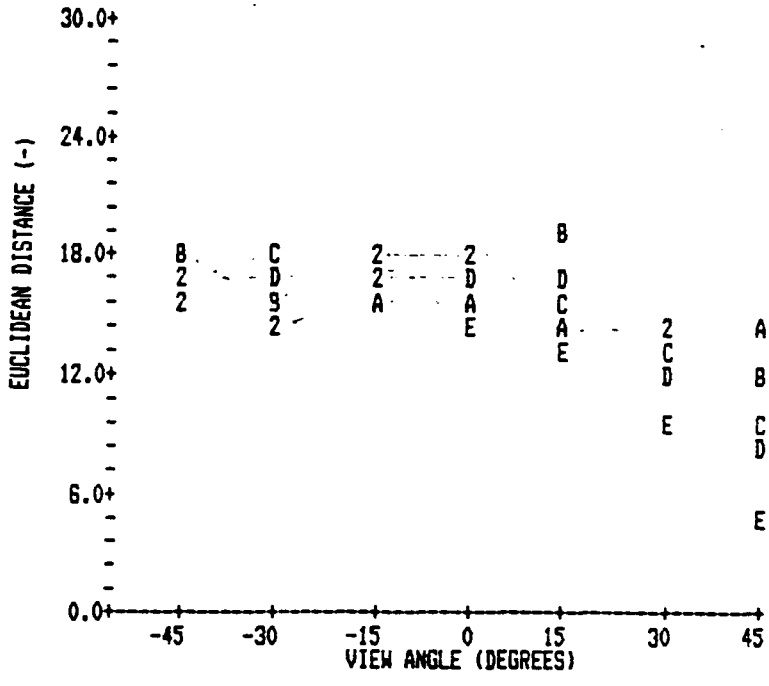
EUCLIDEAN DISTANCE (-)
30.0+
24.0+
18.0+
12.0+
6.0+
0.0+
-45
-30
-15
0
15
30
45
VIEW ANGLE (DEGREES)

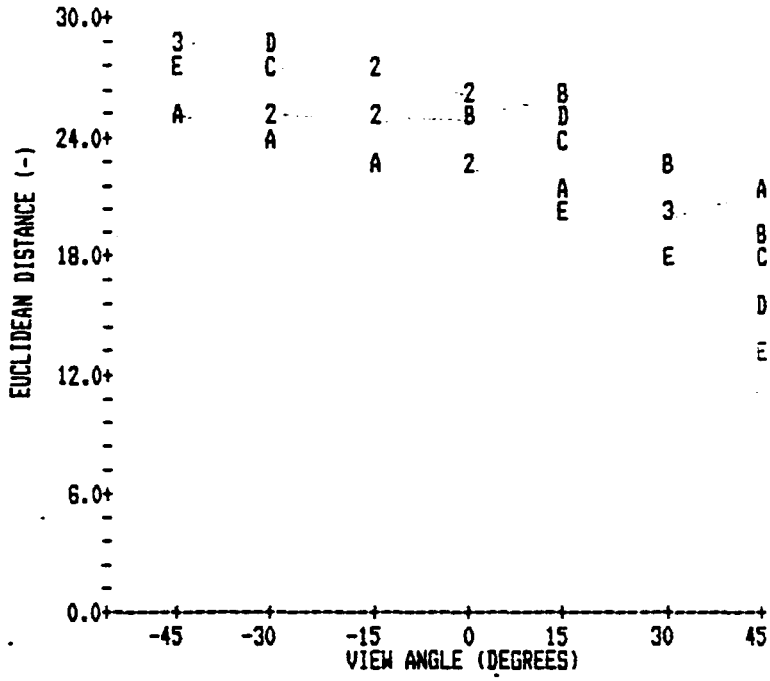
30.0+
24.0+
18.0+
12.0+
6.0+
0.0+
EUCLIDEAN DISTANCE (-)
-45
-30
-15
0
15
30
45
VIEW ANGLE (DEGREES)

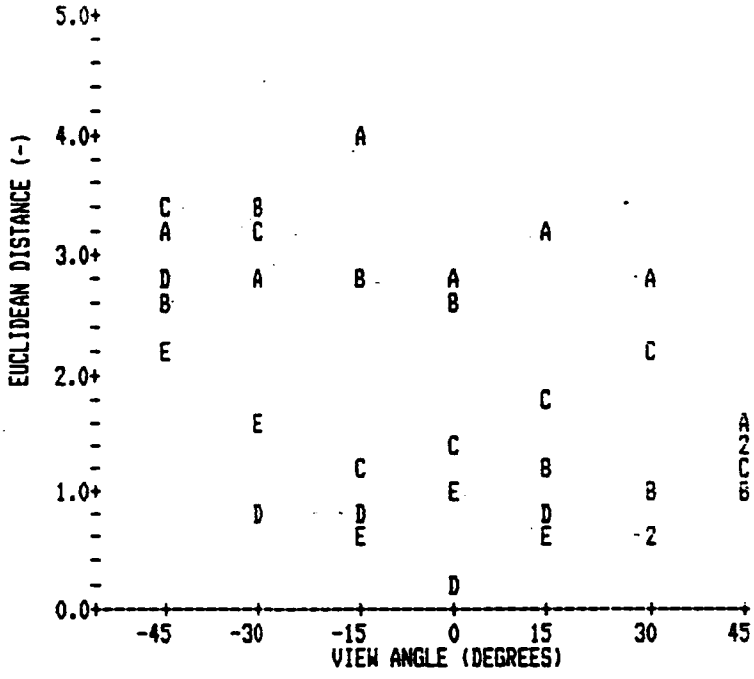
EUCLIDEAN DISTANCE (-)
5.0+
4.0+
3.0+
2.0+
1.0+
0.0+
-45
-30
-15
0
15
30
45
VIEW ANGLE (DEGREES)

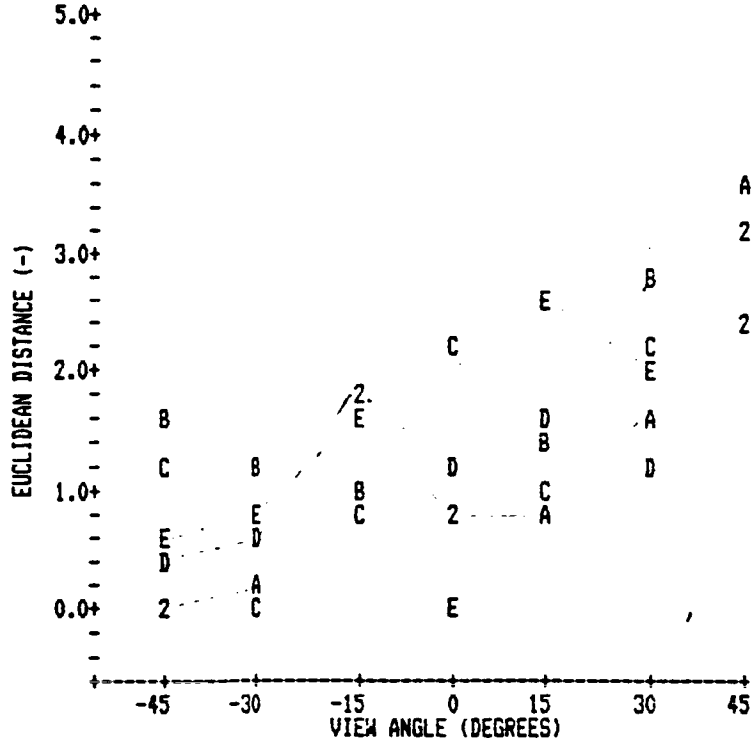
EUCLIDEAN DISTANCE (-)
5.0+
4.0+
3.0+
2.0+
1.0+
0.0+
-45
-30
-15
0
15
30
45
VIEW ANGLE (DEGREES)

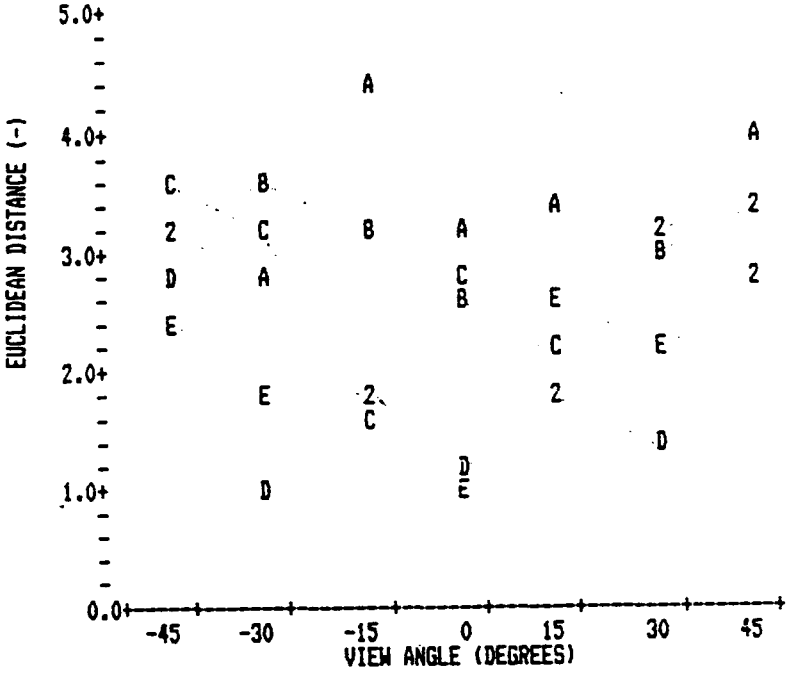
EUCLIDEAN DISTANCE (-)
5.0+
4.0+
3.0+
2.0+
1.0+
0.0+
-45
-30
-15
0
15
30
45
VIEW ANGLE (DEGREES)

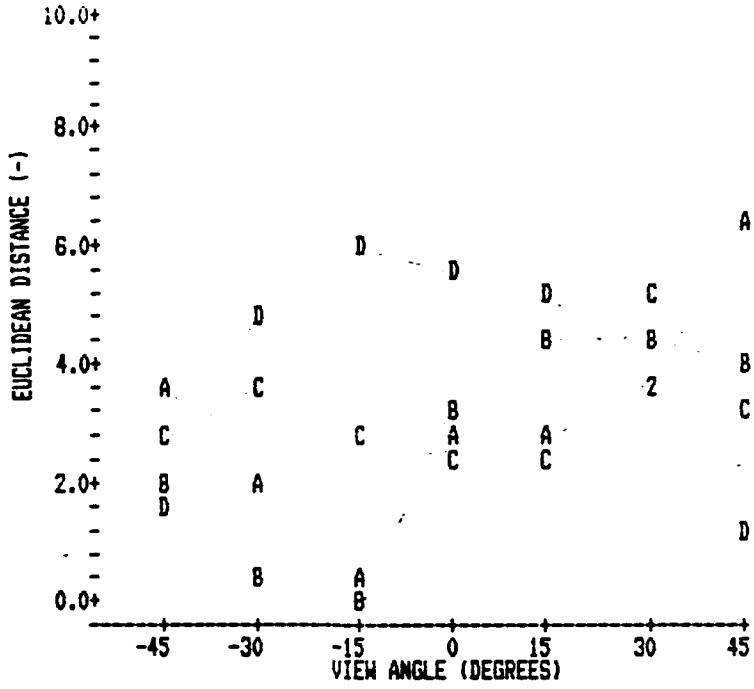
EUCLIDEAN DISTANCE (-)
10.0+
8.0+
6.0+
4.0+
2.0+
0.0+
-45
-30
-15
0
15
30
45
VIEW ANGLE (DEGREES)

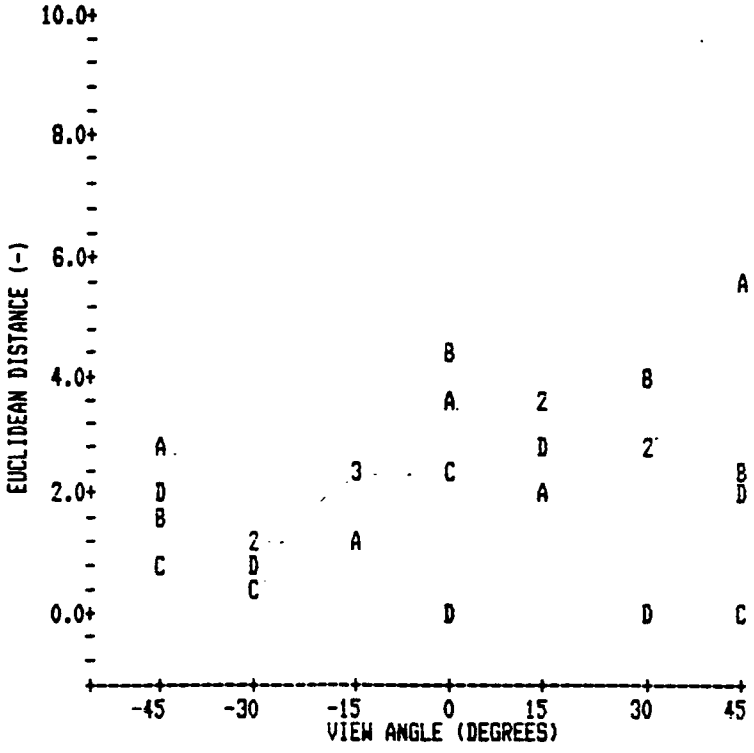
EUCLIDEAN DISTANCE (-)
10.0+
8.0+
6.0+
4.0+
2.0+
0.0+
-45
-30
-15
0
15
30
45
VIEW ANGLE (DEGREES)

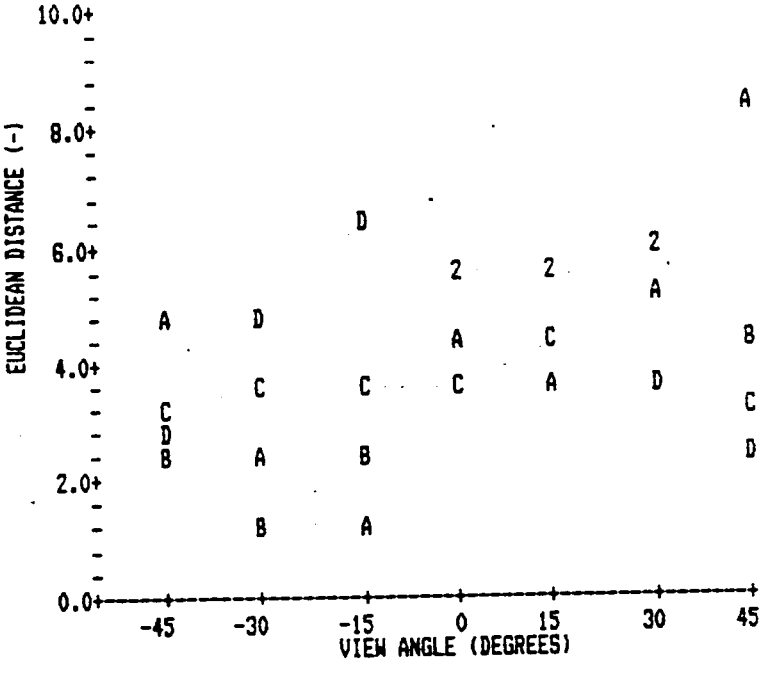
10.0+
8.0+
6.0+
4.0+
2.0+
0.0+
EUCLIDEAN DISTANCE (-)
-45
-30
-15
0
15
30
45
VIEW ANGLE (DEGREES)

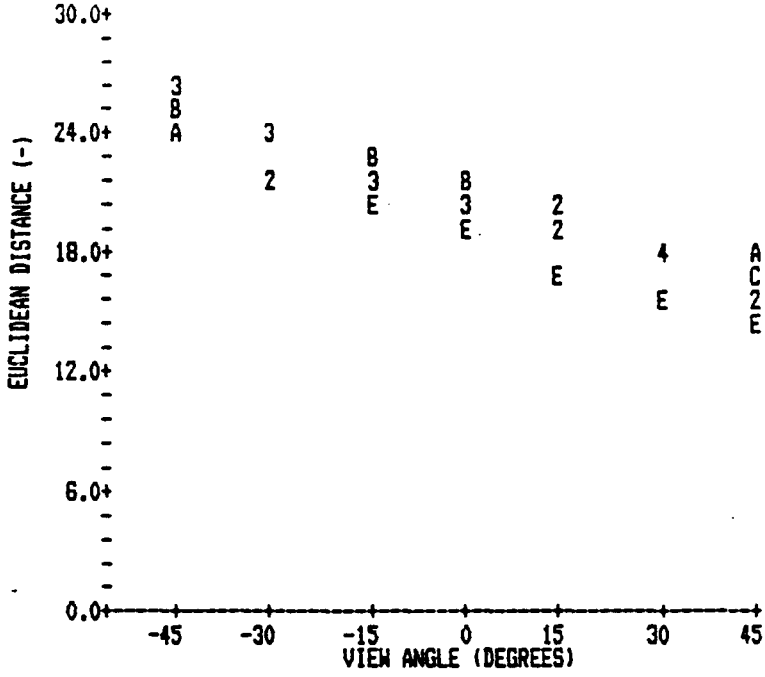
EUCLIDEAN DISTANCE (-)
30.0+
24.0+
18.0+
12.0+
6.0+
0.0+
-45
-30
-15
0
15
30
45
VIEW ANGLE (DEGREES)

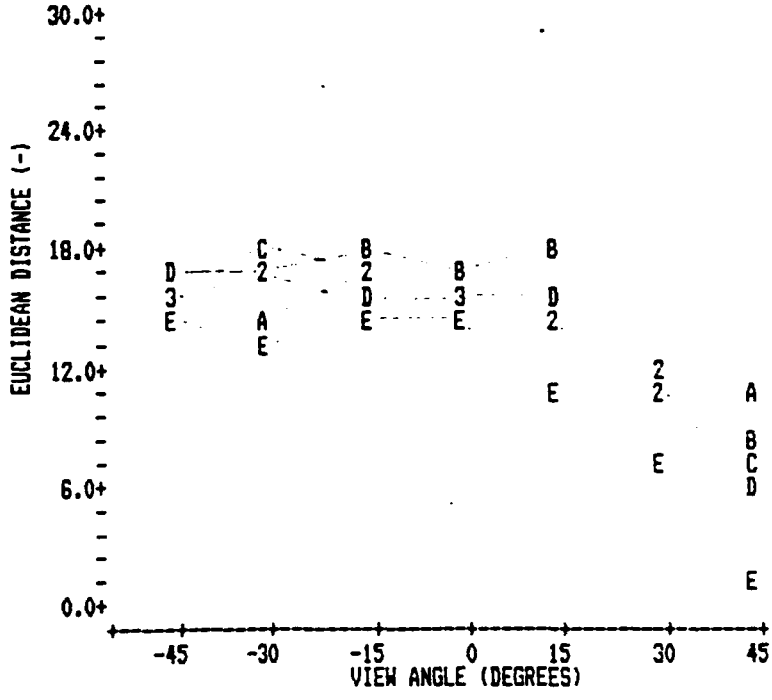
EUCLIDEAN DISTANCE (-)
30.0+
24.0+
18.0+
12.0+
6.0+
0.0+
-45
-30
-15
0
15
30
45
VIEW ANGLE (DEGREES)

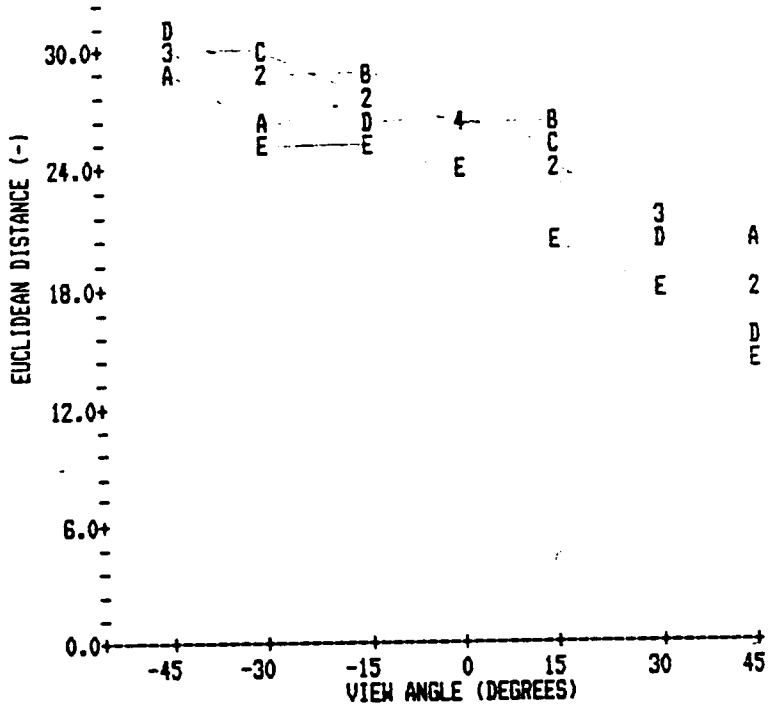
EUCLIDEAN DISTANCE (-)
30.0+
24.0+
18.0+
12.0+
6.0+
0.0+
-45
-30
-15
0
15
30
45
VIEW ANGLE (DEGREES)

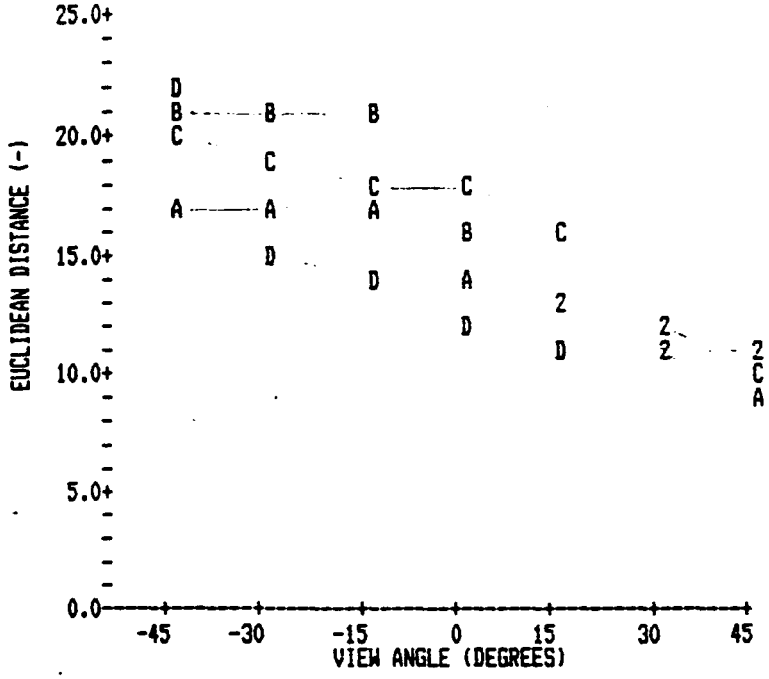
EUCLIDEAN DISTANCE (-)
25.0+
20.0+
15.0+
10.0+
5.0+
0.0
-45
-30
-15
0
15
30
45
VIEW ANGLE (DEGREES)

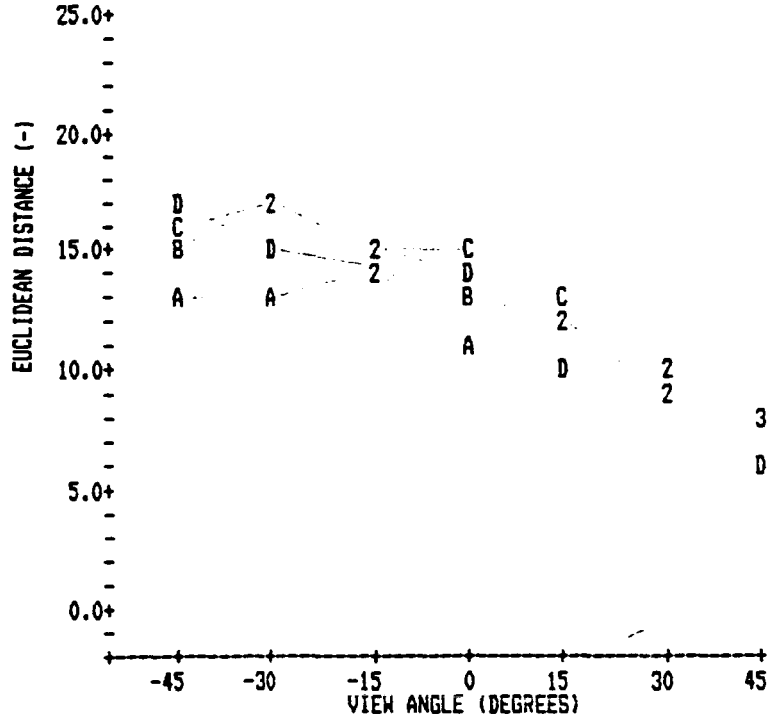
EUCLIDEAN DISTANCE (-)
25.0+
20.0+
15.0+
10.0+
5.0+
0.0
-45
-30
-15
0
15
30
45
VIEW ANGLE (DEGREES)

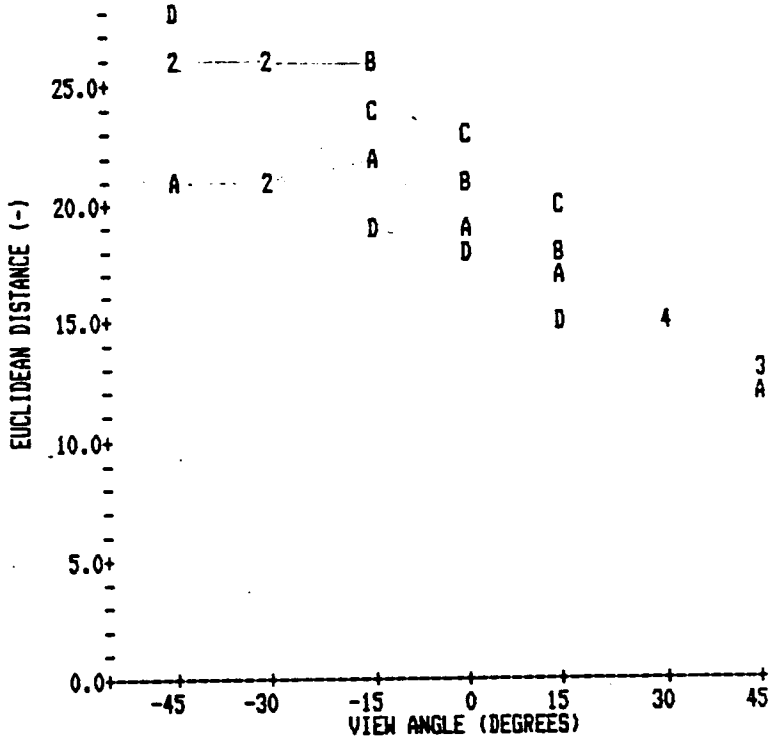
EUCLIDEAN DISTANCE (-)
25.0+
20.0+
15.0+
10.0+
5.0+
0.0+
-45
-30
-15
0
15
30
45
VIEW ANGLE (DEGREES)

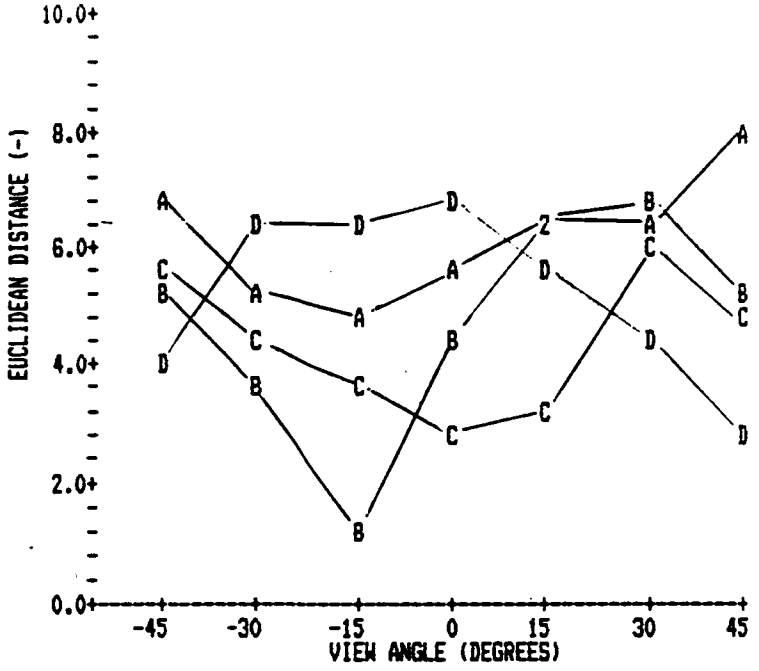
EUCLIDEAN DISTANCE (-)
10.0+
8.0+
6.0+
4.0+
2.0+
0.0+
-45
-30
-15
0
15
30
45
VIEW ANGLE (DEGREES)

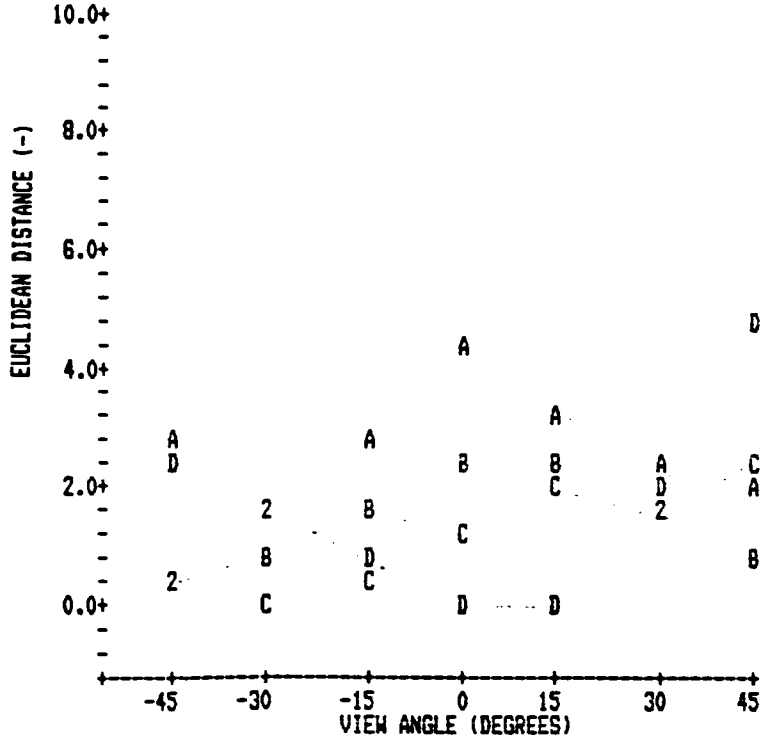
EUCLIDEAN DISTANCE (-)
10.0+
8.0+
6.0+
4.0+
2.0+
0.0+
-45
-30
-15
0
15
30
45
VIEW ANGLE (DEGREES)

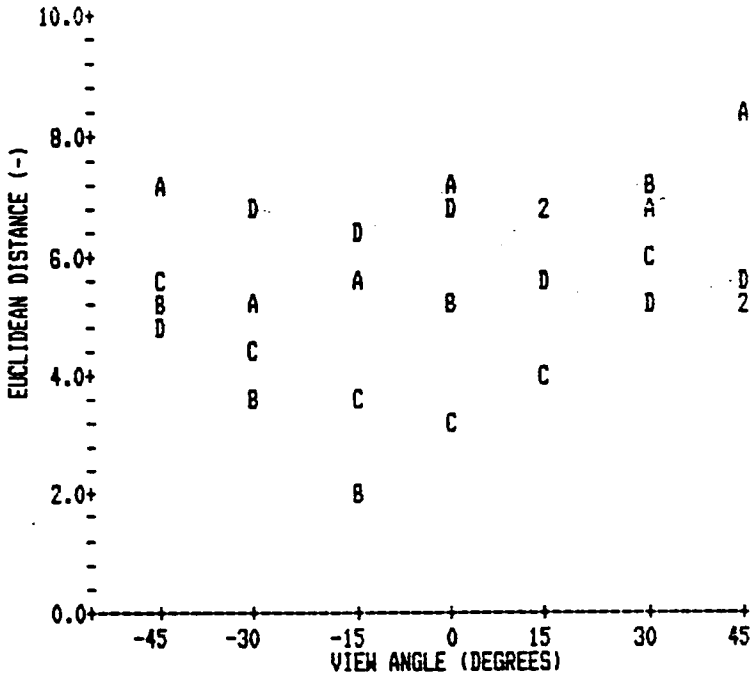
10.0+
8.0+
6.0+
4.0+
2.0+
0.0+
EUCLIDEAN DISTANCE (-)
-45
-30
-15
0
15
30
45
VIEW ANGLE (DEGREES)

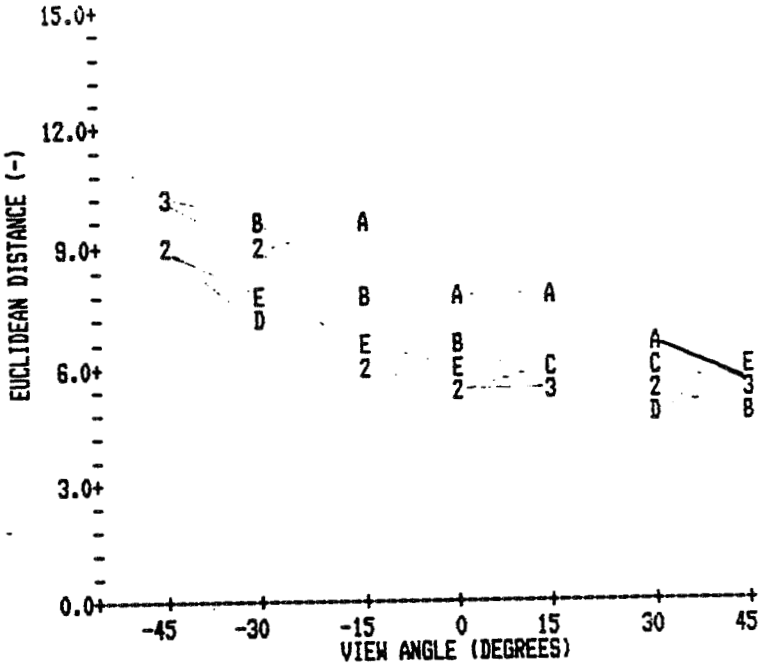
15.0+
12.0+
9.0+
6.0+
3.0+
0.0+
EUCLIDEAN DISTANCE (-)
-45
-30
-15
0
15
30
45
VIEW ANGLE (DEGREES)

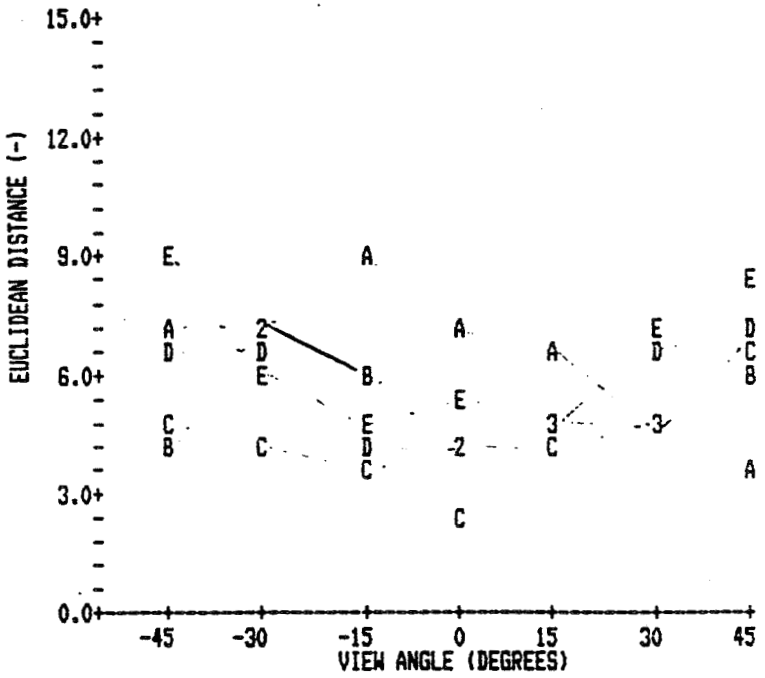
15.0+
12.0+
9.0+
6.0+
3.0+
0.0+
EUCLIDEAN DISTANCE (-)
-45
-30
-15
0
15
30
45
VIEW ANGLE (DEGREES)